



universität
wien

MASTERARBEIT

Titel der Masterarbeit

Age dependent changes
of membrane currents and phagocytic activity
of β -amyloid plaque-associated microglia
in the 5XFAD mouse model of Alzheimer's disease

verfasst von

Natascha Vana, BSc

angestrebter akademischer Grad

Master of Science (MSc)

Wien, 2015

Studienkennzahl lt. Studienblatt:

A 066 834

Studienrichtung lt. Studienblatt:

Masterstudium Molekulare Biologie

Betreut von:

Univ.-Prof. Mag. Dr. Johannes Berger

Table of content

<u>1. Introduction</u>	5
1.1 The central nervous system in neurodegenerative diseases	5
1.1.1 Alzheimer’s disease and the inflammation hypothesis	5
1.2 Mouse models of Alzheimer’s disease.....	7
1.3 General functions of microglial cells.....	9
1.2.1 Microglial characteristics linked to Alzheimer’s disease.....	10
1.2.2 Electrophysiology of microglia.....	11
1.2.2.1 Voltage-gated membrane current densities in microglia	11
1.2.2.2 Purinoreceptors in microglia	12
1.2.3 Phagocytosis in microglia.....	13
1.4. Aim of the project.....	15
<u>2. Material & Methods</u>	17
2.1 Animals	17
2.2 Preparation of acute brain slices	17
2.3 Electrophysiology.....	18
2.3.1 Patch-clamp setup	18
2.3.2 Whole-cell recordings.....	20
2.3.3 Data collection	21
2.4 Phagocytosis assay.....	21
2.4.1 Incubation of acute brain slices with FBS-coated microspheres	21
2.4.2 Staining of fixated brain slices	22
2.4.3 Confocal laser scanning microscopy	23
2.4.4 Data collection	23
2.5 Statistical analysis.....	23
<u>3. Results</u>	25
3.1 Patch-clamp recordings	25
3.1.1 Membrane properties of microglial cells.....	25
3.1.1.1 Membrane current density in microglial cells of 5XFAD mice	25
3.1.1.2 Membrane current densities in microglial cells of WT mice.....	26
3.1.1.2 Comparison of membrane properties of microglial cells in age matched 5XFAD and WT mice	28

3.1.2 Purinergic receptor agonist induced currents	31
3.1.2.1 Differences in purinergic current responses at different ages.....	31
3.1.2.1.1 ATP responses at different ages in 5XFAD and WT mice	32
3.1.2.1.2 BzATP responses at different ages in 5XFAD and WT mice.....	33
3.1.2.1 Differences in purinergic responses between 5XFAD and WT mice	36
3.2 Phagocytosis in microglia of 9-month-old 5XFAD mice is reduced	40
<u>4. Discussion</u>	43
4.1 Microglia in the 5XFAD mouse get increasingly activated with age	43
4.2 Microglia in the 5XFAD mouse demonstrate a decreased responsiveness to purinergic signaling with age	45
4.3 Microglia of 5XFAD experience an impairment in phagocytosis with age	46
4.4 Microglia in the 5XFAD might undergo senescence	47
<u>5. References</u>	50
<u>6. Abstract</u>	59
<u>7. Zusammenfassung</u>	60
<u>8. List of abbreviations</u>	62
<u>9. Acknowledgements</u>	65
<u>10. Curriculum Vitae</u>	67

1. Introduction

1.1 The central nervous system in neurodegenerative diseases

Neurodegeneration is the progressive dysfunction and loss of neurons and synapses in the central nervous system (CNS). There are several diseases associated with the occurrence of neurodegeneration like Alzheimer's disease (AD) and Parkinson's disease. A common hallmark to acute and chronic neurodegeneration is immune activation, known as neuroinflammation. Under normal conditions inflammatory processes within the CNS are kept on a very restricted level and especially microglia and astrocytes, but also neurons contribute to an anti-inflammatory environment. When pathogens have overcome the blood-brain barrier or tissue is damaged or stressed their highly conserved structural motifs act on pattern-recognition receptors (PRRs) of local CNS cells, which elicits innate immune responses. (Amor et al., 2010) During this process pro-inflammatory cytokines and chemokines are secreted especially by microglia, which can damage neurons in two ways. Neurons can be damaged through the release of toxic mediators such as cytokines and free radicals on the one hand and through the recruitment of cells of the adaptive immune system on the other hand. (Rock et al., 2004) In this way the immune privilege of the CNS is lifted and the brain becomes infiltrated by monocytes, neutrophils and t cells (Amor et al., 2010). Eliminating pathogens, clearing debris and stimulating tissue repair inflammation is an initially beneficial process, which in a chronic state contributes actively to neuronal damage and degeneration (Gao & Hong, 2008).

1.1.1 Alzheimer's disease and the inflammation hypothesis

One of the most prominent neurodegenerative diseases is AD. It is the most common form of dementia among older adults affecting 50-75% of 44 million demented people worldwide (Prince et al., 2014). It is an irreversible, progressive brain disorder characterized by cognitive and functional deficits and memory loss. On the cellular level this disease is marked by the presence of insoluble A β plaques (senile

plaques) and by intracellular neurofibrillary tangles containing hyperphosphorylated tau protein. (Tanzi & Bertram, 2005)

Although the first description of AD by Alois Alzheimer goes back to the early 20th century (Alzheimer, 1907) it took 90 years until a link between AD and inflammation was suggested. The identification of activation factors for the complement system as well as thrombin involved in the coagulation system in senile plaques gave first hints that extracellular deposit of A β is connected to the activation of the immune system (Akiyama, 1994). Since then several studies have supported the theory that inflammation presented an integral part of the disease, which not only precedes disease onset (Tarkowski et al., 2003) but could also be triggered by systemic inflammation. In a seminal study prenatal mice exposed to immune challenges developed an AD-like neuropathology during aging, which was even aggravated when they were exposed to a second immune challenge as adults (Krstic et al., 2012).

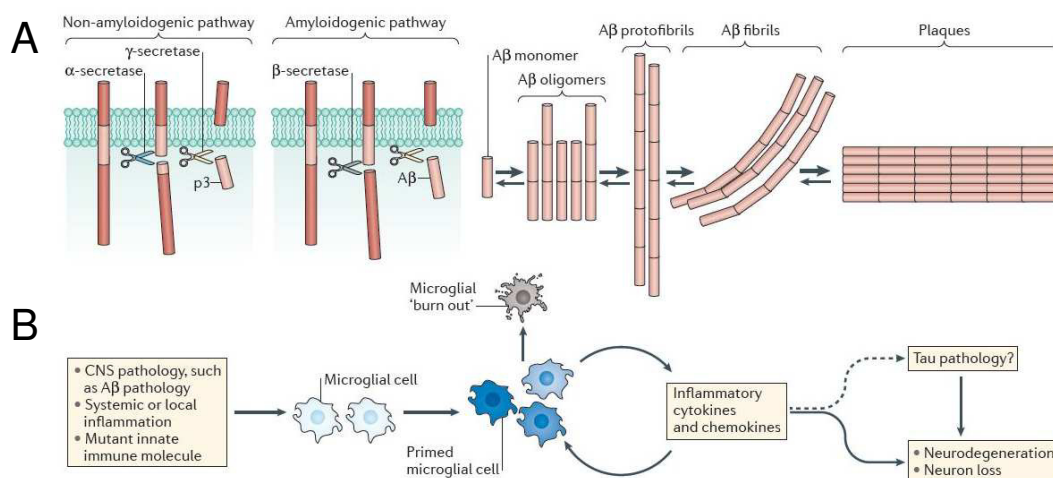


Fig.1. Processing pathways for the APP and its involvement in AD pathology. In AD the physiological processing of APP by means of the α - and γ -secretase (non-amyloidogenic pathway) is superseded by the amyloidogenic pathway when then cleavage of the β -secretase precedes the γ -secretase. A β monomers can aggregate and form deposits in form of A β plaques. (A) The A β protein is only one of several factors, which have to act in concert to cause AD. A β and other triggers prime microglia making them susceptible to activation. Differently colored microglia reflect different states of activation. Activated microglia secrete inflammatory cytokines and chemokines, which react on other microglia possibly aggravating the pathology. The inflammatory environment promotes neurodegeneration and maybe tau pathology. Some of the activated microglia experience a shift to a "burn out"-like state, in which they are dysfunctional. (B) Taken from Heppner et al. (2015). Immune attack: the role of inflammation in Alzheimer disease. *Nature Reviews Neuroscience*, 16(6), 358–372.

Microglia, the resident macrophages of the central nervous system were detected to cluster around senile plaques in AD already in the 1920s (Hortega et al., 1927 in Mrak, 2012), but their important role in AD pathology was recognized only decades later.

Nowadays microglia are assumed to be primed by various alterations in the CNS challenging the immune system like systemic or local inflammations, mutations in genes encoding innate immune molecules or pathological protein aggregates (Fig. 1B). The primed microglial cells can then be activated by a second immune challenge and this activation state is maintained by the constant accumulation of A β . Activated microglia secrete cytokines and chemokines, which again activate other primed microglia. (Heppner et al., 2015) The functional state of microglia during AD progression is marked by three stages. At first activated microglia clear A β deposits, release growth factors and anti-inflammatory cytokines and phagocytose damaged cells. While this activity is generally considered as beneficial for the brain, a shift to a more cytotoxic phenotype occurs at later stages. At this point in AD microglia release proinflammatory cytokines, which affects the homeostasis of the whole brain causing neuronal loss and tissue damage. Chronic exposure to inflammatory stimuli, for example A β aggregates, damage microglia which manifests itself in reduced phagocytic capacity, reduced motility and altered cytokine production. While this dysfunctional state is reversible, microglia exposed to chronic activation as in older AD patients can become irreversibly dysfunctional, referred to as senescent cells. (Prokop et al., 2013)

1.2 Mouse models of Alzheimer's disease

Mouse models present an indispensable tool in research and especially regarding investigations of AD. Most obviously human material is generally obtained post mortem from AD patients which allows no investigations regarding the development of the disease.

As one of the two major hallmarks in AD the generation of insoluble deposits of β -amyloid (A β) has been in the focus of research on the genetic basis of AD pathology. Nowadays it is well known that the A β peptide is derived from the APP (amyloid precursor protein), which undergoes proteolytic processing (Fig.1B). Under

physiological conditions this transmembrane protein is cleaved by the α - and then the γ -secretase secreting a peptide called p3 (the non-amyloidogenic pathway). However, A β is generated when the first proteolytic enzyme cleaving APP is the β -secretase instead of the α -secretase (the amyloidogenic pathway) and released in the cytosol where it accumulates in senile plaques. (Haass et al., 2012)

AD can be classified in early-onset Alzheimer's Disease (EOAD) or late-onset AD (LOAD) depending on whether the disease emerges before or after a certain age, most commonly at the age of 60. Several mutations in genes involved in APP processing namely APP and the presenilin genes (PSEN1, PSEN2) were linked to EOAD, but not LOAD. Given this, EOAD is most commonly associated with a hereditary form of AD and therefore also referred to as early-onset familiar Alzheimer's Disease (EOFAD). While studies investigating the relation between mutations in APP and PSEN1 have yielded ambiguously results, a polymorphism in the gene encoding Apolipoprotein E (APOE) has been clearly defined as a LOAD susceptibility gene. (Tanzi et al., 2005) Since mutations in the genes encoding APP and the presenillins are fully penetrant, they provided the foundation for the engineering of a multitude of AD mouse models (for an overview on the different AD mouse models have a look at www.alzforum.org/research-models, 01.09.2015).

Consequently the majority of mouse models carry mutations in genes for APP, presenilin 1 (PS-1) and/or 2 (PS-2), from which the latter two are subcomponents of the γ -secretase. The mouse model employed in this study, the 5XFAD mouse (Oakley et al., 2006) was generated with five AD-related mutations, the Swedish, Florida (I716V) and London (V717I) mutations in human APP (hAPP) and the M146L and L286V mutations in PS-1. The 5XFAD mouse develops an AD-like phenotype more rapidly than other AD mouse models. At 1,5 months of age the first A β plaques appear, which is followed by gliosis at 2 months of age. Further signs for cognitive impairment become apparent at 4 to 5 months of age, while significant neuronal and synaptic loss starts at around 9 months of age.

1.3 General functions of microglial cells

Microglia belong to a group of mononuclear phagocytes, which serve as the resident immune system in the CNS. These cells derive from the yolk sac and invade the brain at an early stage during embryonic development (Pont-Lezica et al., 2011). After invading the brain they are equally distributed and constantly scan the surrounding area for danger signals. Physiological microglia exhibit a ramified morphology, which allows them to stretch out their moving processes in the surrounding. If microglia sense disturbances they get activated adopting a macrophage phenotype during which they express biological markers distinct from their physiological state. Reactive microglia become amoeboid shaped, migrate to the site of injury and proliferate. (Kettenmann et al., 2011)

In order to recognize changes in their environment microglia are equipped with an array of different receptors for neurotransmitters and neuromodulators, cytokines or chemokines (Kettenmann et al., 2011). Pathogens as well as damaged or stressed tissue express highly conserved structural motifs, pathogen-associated molecular patterns (PAMPs) or danger-associated molecular patterns (DAMPs). Both bind to conserved PRRs, which upon activation elicit innate immune responses. One class of PRRs, the Toll-like receptors (TLRs) are highly abundant in microglia making them responsive not only to invading microorganisms, but also to endogenous danger signals. However, danger signals can act on a variety of microglial cell membrane receptors like cytokine/chemokine receptors, scavenger receptors, purinogenic receptors and many others (Rock et al., 2004). Danger signals include heat shock proteins, uric acid, chromatin, adenosine and adenosine 5'-triphosphate (ATP). Furthermore, fibrinogen and aggregated, modified or misfolded proteins such as A β , α -synuclein and microtubule associated protein-tau are recognized by microglia causing the cell to secrete inflammatory mediators. (Amor et al., 2010)

In the brain microglia exert a multitude of different immune-modulatory functions. Depending on their activation state they can secrete pro- or anti-inflammatory factors and phagocytose pathogens, cell debris and pathological accumulations of extracellular molecules. Moreover they can release cytotoxic substances, act as antigen-presenting cells and promote repair of neural tissue via neurotrophic factors. (Kettenmann et al., 2011) In the following the rapid activation

and response of microglia to damage in the brain with respect to electrophysiological changes and phagocytic activity and their roles in AD will be discussed in more detail.

1.2.1 Microglial characteristics linked to Alzheimer's disease

The central hallmark of AD is the presence of extracellular A β peptide deposits, which can damage neurons directly or via consecutive effects by activating the innate immune system (Salminen et al., 2009). The overwhelming mass on AD publications has generated a very heterogeneous nomenclature for the different appearances of amyloid aggregates. A cross differentiation can be made between diffuse and dense-core plaques, from which the later is the one mainly associated with reactive microglia accumulation (McGeer et al., 1994; Ohgami et al., 1991). Reactive oxygen species (ROS) for example were found to be associated with dense-core plaques, but not with diffuse plaques *in vivo* and *in situ* (McLellan et al., 2003). Activation of microglia is inherently linked to chemotaxis (Rogers et al., 2001; Lue et al., 2001b), which explains why microglia are consistently found in close proximity to A β plaques in humans as well as animal models of AD (Bacsikai et al., 2001; Frautschy et al., 1992; Frautschy et al., 1998; Itagaki et al., 1964; Terry et al., 1964) (Fig.2).

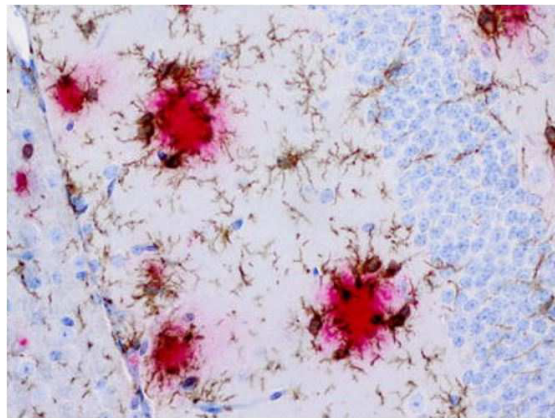


Fig.2. Microglia clustered around A β plaques demonstrate an activated morphology in an AD mouse model. Immunohistochemistry was employed to detect microglia with Iba1 depicted in brown, plaques were labeled by means of an antibody directed against A β , 17-24 (4G8) presented in red. Figure taken from Prokop et al. (2013). Microglia actions in Alzheimer's disease. *Acta Neuropathologica*, 126(4), 461–477.

At the site of injury or inflammation unusual material like A β is recognized by reactive microglia via PPRs inducing the release of inflammatory mediators from these

cells (Salminen et al., 2009; Wilkinson et al., 2012). Thus increased levels of different immune molecules such as interleukin (IL)-1, IL-6, tumor necrosis factor- α (TNF- α), MIP-1 β , complement proteins and oxygen radicals are found in the brains of AD patients (Salminen et al., 2009). Support for the link between A β and inflammation comes from a study (Lue et al., 2001a), in which pre-aggregated A β was added to isolated microglia from brains of AD patients. Upon treatment levels of pro-IL-1b, IL-6, TNF- α , monocyte chemoattractant protein-1 (MCP-1), macrophage inflammatory peptide-1a (MIP-1a), IL-8, and macrophage colony-stimulating factor (M-CSF) were significantly increased.

1.2.2 Electrophysiology of microglia

Aside from cytomorphological criteria and immunological markers there is growing evidence that microglial activation and their ion channel expression are strongly intertwined in neurodegenerative diseases (Skaper, 2011).

1.2.2.1 Voltage-gated membrane current densities in microglia

Microglia *in vitro* are characterized by a voltage-dependent, inwardly rectifying K⁺ current (Kettenmann et al., 1990). Exposing cultured microglia to proinflammatory stimuli an additional outward K⁺ current can be seen (Nörenberg et al., 1992). However, electrophysiological recordings of cultured microglia were found to differ from acute brain slices (Boucsein et al., 2000). Under normal conditions microglia *in situ* were attributed to have very small voltage-gated membrane currents (Boucsein et al., 2003; Boucsein et al., 2000). Upon injury or pathology microglia have been found to undergo changes in their expression of voltage-gated potassium channels. Facial nerve axotomy in rats demonstrated that shortly after a lesion microglia express predominantly inward rectifying channels, which are later accompanied by outward rectifying channels. These voltage-gated currents seem to diminish in amplitude over time until the cells again exhibit only minor currents similar to ramified microglia. (Boucsein et al., 2000) The same activation pattern with varying time periods was detected in murine microglia after induction of ischemic stroke (Lyons et al., 2000) and in a mouse model of status epilepticus (Avignone et al., 2008). These studies suggest

that a possible activation of microglia is accompanied by a change in their membrane properties, and can be seen for example in their voltage-gated membrane currents.

Considering the literature indicating that microglia get activated by the A β protein, it is likely that a similar electrophysiological pattern could be found in the AD pathology. One hint comes from a study showing that microglia get activated and display Ca²⁺- and voltage-gated K⁺ currents as well as inwardly rectifying currents upon stimulation with A β oligomers (Maezawa et al., 2011). Another study correlated A β concentrations with increasing outward rectifying K⁺ currents in cultured microglia (Chung et al., 2001). Whether increased membrane currents can also be found in a more physiological setting has not been investigated yet.

1.2.2.2 Purinoreceptors in microglia

A lot of different substances can exert a modulating role on microglial functions, but one of the most important signaling molecules for microglial activation are purines and pyrimidines influencing ionic current, membrane potential, gene transcription, production of inflammatory mediators and cell survival (Sperlágh et al., 2007). Originally purinoreceptors were classified in the adenosine-responsive P1 receptors and the ATP-responsive P2 receptors. Nowadays three classes of purinoreceptors are distinguished, the metabotropic P1 family, the metabotropic P2Y family and the ionotropic P2X family of receptors. ATP and its derivatives are the main purinergic signaling molecules, the first being the only endogenous ligand for P2X channels, causing a non-selective cation current (Yang et al., 2012). In the brain ATP acts not only as a neurotransmitter, but also as an universal danger signal readily released by cells upon mechanical stimulation and energy deprivation. Moreover, inflammatory mediators, cellular damage or changes in the ionic environment can also cause ATP release. (Sperlágh et al., 2007)

As the guardians of the brain microglia are equipped with a whole array of purinergic receptors allowing them to sense disturbances and react to them (Davalos et al., 2005). ATP evokes electrophysiological responses in microglia in some cases triggering both, a P2Y receptor-mediated outward rectifying K⁺ current and/or a P2X receptor-mediated inward cationic current (Boucsein et al., 2003). Moreover P2X and

P2Y receptors expressed in microglia have been shown to control migration, phagocytosis and cytokine release (Hide et al., 2000; Koizumi et al., 2007; Ohsawa et al., 2007). Since purinoreceptors are highly abundant in microglia purinergic signaling was implicated to contribute to inflammation and CNS diseases such as AD (Skaper et al., 2010).

Among the purinergic receptors on microglia the P2X7 receptor gained attention when P2X7 receptor-positive microglia were detected to cluster around A β plaques in the Tg2576 AD mouse model (Parvathenani et al., 2003). In human material P2X7 immunoreactivity was detected around senile plaques and colocalized to microglia (McLarnon et al., 2006). Several *in vitro* studies linked the P2X7 receptor to the pathology of AD. Preincubation of microglia with A β peptide resulted in the secretion of IL-1 beta (IL-1 β) upon stimulation of the P2X7 receptor with the P2X7-specific agonist 2',3'-(benzoyl-4-benzoyl)-ATP (BzATP) (Rampe et al., 2004). A β was shown to induce increased expression of P2X7 receptors in microglia *in vitro* and *in vivo* (McLarnon et al., 2006). Furthermore the P2X7 receptor was proposed to be required for microglial activation when A β induced activation markers were detected in microglia from wild-type (WT) mice, but not from P2X7^{-/-} mice (Sanz et al., 2009).

It has been noted that microglia are very heterogenous regarding the purinergic receptors they are equipped with (Boucsein et al., 2003). Several investigations point to the fact that the purinergic system in microglia is highly plastic depending on the activation state (Kettenmann et al., 2011). In a mouse model of status epilepticus (SE) the induction of seizures lead to the upregulation of several purinergic receptors (including the P2X7 receptor) in microglia (Avignone et al., 2008).

Taken together these findings suggest that the purinoreceptive system in microglia plays a pivotal role in AD pathology and electrophysiological responses to ATP application can be used to infer the activation state of microglia.

1.2.3 Phagocytosis in microglia

As the brain's professional phagocytes microglia can not only recognize and respond to A β , they are also able to incorporate this peptide. Fibrillary A β aggregates can be taken up by mouse microglia primary cultures via scavenger receptors into endosomes (Paresce et al., 1996). *In vitro* studies with rat microglia demonstrated that

they intracellularly accumulated A β peptide, while culturing the same cells on unfixed slices from AD patients lead to only marginal A β uptake (Ard et al., 1996). Furthermore it was shown that cultures of rat microglia were able to degrade soluble A β in the medium as well as artificial deposits of synthetic A β (Shaffer et al., 1995).

The clearance of A β through microglia was demonstrated even *in vivo* when fibrillar and soluble A β peptides were injected into rat brains (Weldon et al., 1998). In another experiment Frautschy et al. (1992) injected senile plaque cores isolated from AD brains into the rat cortex and hippocampus. In the time course of one month amoeboid microglia had surrounded the amyloid injection phagocytosing the peptide.

By means of *in vivo* imaging it was shown that senile plaques can be cleared in a transgenic (TG) mouse model of AD upon immunization with A β peptide (Bacskai et al., 2001). Primary cultures of microglia cultured with sections of the PDAPP mouse model or tissue of AD patients in the presence of A β antibodies demonstrated that in both conditions microglia phagocytosed and degraded A β (Bard et al., 2000). However, given the only marginal engagement of the adaptive immune system in AD (Heppner et al., 2015) these animal experiments do not model the whole spectrum of human AD pathology.

Anyway the question arises why microglia obviously fail to successfully clear A β deposits despite their constant activation and their principal capability to incorporate and digest A β . One factor explaining the apparent contradiction could be the time microglia are exposed to the putatively damaging A β peptide having an adverse effect on their functioning. During a 12-day period Chung et al. (1999) showed that cultured microglia of WT mice indeed incorporated fibrillary as well as soluble forms of A β and started to degrade it, but this degradation is only partial and a considerable amount of A β was even released again.

Indeed an impairment in microglial phagocytosis *in situ* was demonstrated in two different AD mouse models, which was accompanied by increasing levels of A β plaques in the brain (Krabbe et al., 2013). A finding which might explain why microglial depletion in an AD mouse model showed no influence on A β levels (Grathwohl et al., 2009).

This suggest that microglia experience some kind of impairment in their phagocytic functions, which could be possibly linked to the increasing accumulation of

A β peptides in the brains of AD patients. However, the phagocytic capacities of microglia in an AD mouse model have never been correlated to the activation of voltage-gated membrane currents in these cells.

1.4. Aim of the project

The absolute need to investigate AD follows from the already very high prevalence set to more than triple by 2050 (Prince et al., 2015). Despite the very huge amount of research already conducted in this field, AD is still incurable. The complexity and diversity of this disease still challenges researchers worldwide. Since the emergence of the inflammation hypothesis in AD research, a lot of investigations have been conducted regarding the involvement of microglia in its pathophysiology. While this research has mainly focused on immunological markers, the electrophysiological properties of microglia in the AD context have been neglected.

To fill that gap microglia in acute slices derived from the 5XFAD mouse model were investigated in this study by means of the patch-clamp technique. Aberrant membrane currents have been already reported for other diseases providing good reason that microglia exhibit a distinct membrane current pattern in an AD mouse model, which should not be found in microglia of healthy mice. Given that microglia can recognize and react to A β in a way generally assumed as activation, these currents should be found in microglia in close proximity to A β plaques. Furthermore the electrophysiological responses of microglia to ATP and BzATP application were assessed in the same mouse model, which were expected to be significantly different from those in WT animals. To determine the changes during pathophysiology, three different age stages, namely 1, 3 and 9 months had been selected for experimental analyzes. Possible alterations in microglial function, were detected employing a phagocytose assay *in situ* at 3 and 9 months of age.

Therefore the aim of this master's project is to electrophysiologically characterize microglia in brain slices of AD mouse models by means of the patch-clamp technique. To link the activation of membrane currents to the functional activity of microglia, the data gained from the patch-clamp technique were correlated with the phagocytic capacities of microglia in the 5XFAD mouse model. By also studying changes in phagocytosis at corresponding ages, the dichotomy between an overactivation and a dysfunction of microglia in the neurodegenerative processes of an AD mouse model was investigated.

2. Material & Methods

2.1 Animals

For the present work the 5XFAD mouse model for AD (Oakley et al., 2006) based on C75BL/6 mice was employed. To detect microglia homozygous MacGreen mice expressing enhanced green fluorescent protein (EGFP) under control of the c-fms promoter (Sasmono et al., 2003) were crossbred with 5XFAD mice. Mating homozygous MacGreen mice with heterozygous 5XFAD yielded a constant supply of TG and WT animals expressing green fluorescent cells of the microglia/macrophage lineage. Mice were kept and bred at the local animal facility at a regular light cycle of 12:12 hours light:dark with food and water supply *ad libitum*. Mice were maintained and experiments were conducted in accordance with guidelines of the Committee on the Ethics of Animal Experiments in Berlin (LaGeSo). Genotyping of mice was confirmed by PCR. For experimental procedures male and female mice were used at 1, 3 or 9 months of age.

The c-fms gene encodes the receptor for the M-CSF, also known as colony-stimulating factor 1 (CSF-1). This protein regulates the survival, proliferation and differentiation of monocytes to macrophages. (Stanley et al., 1997) Consequently, no distinction can be made between the brain resident macrophages, namely microglia and bone-marrow derived mononuclear phagocytes invading the brain in disease. Although macrophages were shown to infiltrate the brain in an AD mouse model, only 6% of them were found to be associated with bone-marrow derived macrophages (Malm et al., 2005). The cells found around A β plaques can thus be considered to be brain residential phagocytes, namely microglia. Therefore from this point on they will be referred to as microglia despite being aware of some kind of "contamination" of macrophages.

2.2 Preparation of acute brain slices

Animals were euthanized by cervical dislocation followed by decapitation. The scalp was removed along the sagittal axis to expose the skull. The cranial bone was then dismantled by lateral incisions on each side and one consistent cut along the

sagittal suture. After removing the skull with tweezers the brain was scooped out with a spoon. After removal the brain was washed in an ice-cold buffer of artificial cerebrospinal fluid (ACSF) containing 134 mM NaCl, 2.5 mM KCl, 1.3 mM MgCl₂, 2 mM CaCl, 1.26 mM K₂HPO₄, 26 mM NaHCO₃, 10 mM glucose (pH 7.4) and saturated with carbogen gas (95% O₂, 5% CO₂). Hereafter the cerebellum was cut off from the brain with a razor blade and the brain was mounted with superglue (UHU) on the specimen plate of the vibratome (Leica). A fixated agar block served as a supporting pillar to the brain during sectioning. The magnetic holder with the brain was placed in the buffer tray of the vibratome containing now the ice-cold buffer. The most anterior part was quickly cut off and 250 µm thick coronal slices were cut for electrophysiological recordings and whereas 130 µm thick sections were used for phagocytosis assays.

2.3 Electrophysiology

In order to determine the membrane properties of cortical microglia associated with Aβ plaques in the 5XFAD mouse model, 1, 3 and 9 months old TG and WT mice were analyzed with the patch-clamp technique.

2.3.1 Patch-clamp setup

The setup for electrophysiological recordings consisted of an upright light microscope (Axioskop, Zeiss), which was mounted on an optical table (Newport). The optical table was enclosed by a Faraday cage to avoid any interference of the recording by electric fields. To visualize fluorescent dyes and the EGFP a polychromator was used as an alternative light source when the light emitting aperture was covered. A camera (Sensicam, PCO) was mounted on the microscope in order to visualize the optical signal on a computer using CamWare (PCO). The slices were fixated in a self-made recording chamber between condenser and objective. This chamber was constantly perfused with ACSF by means of a peristaltic pump (Minipuls 3 Peristaltic Pump, Gilson, France) allowing inflow and drain at the same time. When the slice was transferred to the recording chamber, fixated with a grid and bathed by ACSF at room temperature, the micromanipulator (PatchMan, Eppendorf) was used to position the pipette above the slice.

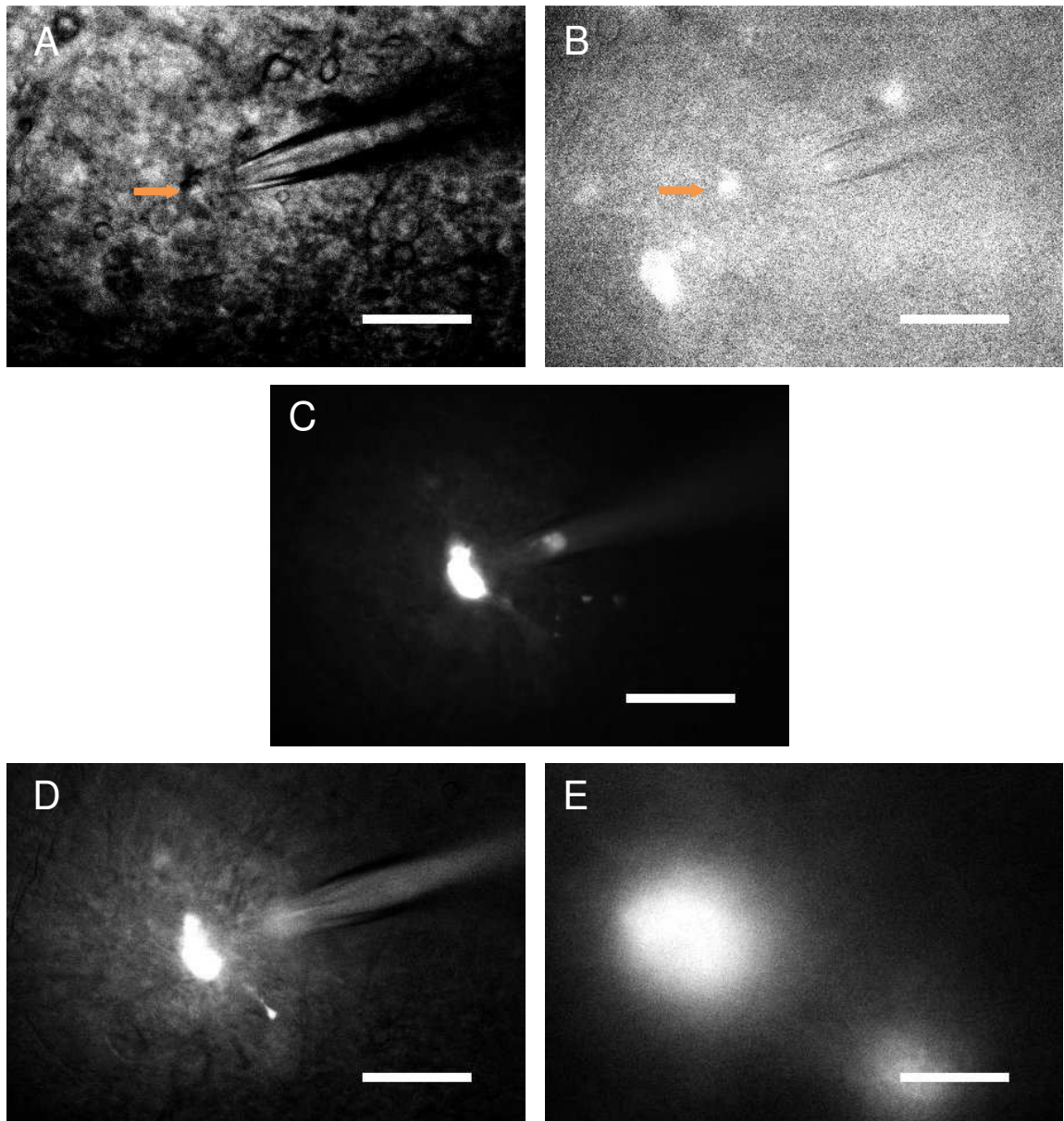


Fig.3. Illustration of the different microscopical views during patch-clamp recordings. Example was taken from a brain slice of a 5XFAD mouse at 9 months of age. Five different pictures from the same area were taken: brightfield (A), green fluorescence to detect EGFP-expressing microglia (B) red fluorescence to check whether the targeted cell was filled with sulforhodamine (C) and therefore successfully patched. Dense-core senile plaques (E) were also detected with red fluorescence, but could be distinguished by their diffuse and round-shaped appearance as well as by their size. and. Note that pictures C, D and E were made in consecutively deeper layers, while pictures A to C were taken from the same level of depth. Arrows indicate position of microglia. Scale bars: 20 μ m.

The pipettes were obtained in advance from borosilicate glass rods heated and torn apart in a micropipette puller (P-97, Flaming/Brown Micropipette Puller, Sutter Instrument). The pipettes had a resistance of 4 to 6 M Ω . Directly before usage the

pipette was filled with intracellular solution containing 130 mM KCl, 2 mM MgCl₂, 0.5 mM CaCl₂, 2 mM Na-ATP, 5 mM EGTA, 10 mM HEPES. In addition Sulforhodamine B (1 mg/ml) was used to control the pipette pressure (Fig.1). The pipette was fastened on the pipette holder and connected to the preamplifier on the micromanipulator. An additional bath electrode was placed at the border of the recording chamber continuously superfused by ACSF. The signal from the preamplifier was then transduced to the patch-clamp amplifier (EPC-9, HEKA) connected to the computer and recorded via the TIDA 5.25 software (HEKA).

2.3.2 Whole-cell recordings

Slices were incubated for 10 minutes in carbogenated ACSF buffer containing 0,001% Thiazine Red R (Sigma-Aldrich) to stain A β plaques (Uchihara et al., 2000) before they were mounted in the patch-clamp chamber. Brain slices were always checked for cortical A β plaques in the 4X objective and cells were patched with a 60X or 63X objective. After identification of A β plaques directly associated green fluorescent microglia in the cortical layers 3 to 6 were patched in a whole-cell configuration (Fig.1). When no plaques were identified microglia were randomly selected within the same layers.

After establishing a gigaohm seal the cell membrane was ruptured at a holding potential of -20 mV and the membrane potential was noted immediately by switching to the current clamp mode. In order to identify voltage gated ion channels and basic electrophysiological cell properties the following protocol was used. Membrane currents were recorded in voltage clamp mode after applying a series of hyper- and depolarizing 10 mV voltage steps ranging from -170 to 60 mV for 50 ms each starting at a holding potential of -40 mV.

To assess the microglial responses in membrane currents to the activation of purinergic receptors ATP (1 mM; Sigma-Aldrich) as well as the P2X7 specific agonist BzATP (0.15 mM; Sigma-Aldrich) were washed in for 1 minute via the bath. A washout time of 5 minutes was used between the two substance applications. In these experiments the cells were depolarized and hyperpolarized between -140 to 60 mV by 20 mV increments for 100 ms. This protocol was repeated every 5 seconds throughout the experiment.

2.3.3 Data collection

The electrophysiological recordings were analyzed using TIDA and Excel. Recordings with a series resistance of above 65 M Ω and/or strong leak currents were discarded. For every sequence the steady-state values, namely the current flowing in the time frame between 60 and 90% of the whole trace length, were used to determine a current-voltage relationship. Furthermore the capacity was calculated from the 10 mV voltage step pulse with TIDA using the Simpson's integration tool. Recorded currents for each cell were normalized to the cell capacitance giving rise to the current density. U-I diagrams were made by plotting the mean current density for each voltage step calculated from all cells measured at one experimental condition. The traces recorded during substance applications were analyzed in TIDA, during which the steady state current for each voltage step repeated every 5 seconds was determined. Excel was used to subtract baseline currents from peak responses to the given substances. In this way the U-I diagrams for BzATP and ATP was established from calculating the mean currents at each voltage step recorded in all the microglia of one condition. All values are given as mean \pm standard error of the mean (SEM).

2.4 Phagocytosis assay

To assess the phagocytic capabilities of microglia in the 5XFAD mice Bright Blue Fluoresbrite Carboxylate Microspheres (Polysciences) with a diameter of 4.5 μm were used. Experiments were conducted in three 9 month old 5XFAD x MacGreen mice, as well as in three age matched WT animals as healthy controls. Moreover the same experiment was done in one 3 month old 5XFAD x MacGreen and two controls.

2.4.1 Incubation of acute brain slices with FBS-coated microspheres

From each mouse six brain sections of 130 μm were cut with the vibratome mentioned above. Slices were stored for 2 hours in normal ACSF at room temperature with constant carbogen supply to let them equilibrate. Fluoresbrite microspheres were incubated with fetal bovine serum (FBS) under constant shaking with 1000 rpm at 22 $^{\circ}\text{C}$. After 30 minutes the suspension was centrifuged for 2 minutes at 3000 rpm to

remove the supernatant. After a washing step in phosphate-buffered saline (PBS), beads were resuspended in Hank's balanced salt solution (HBBS) (10 µl/ml). Brain sections were incubated with the beads solution for 1 hour in a water-saturated atmosphere with 5% carbon dioxide at 37°C. For later orientation a small cut was applied in the left hemisphere. From this time point on samples were kept dark to avoid photo bleaching. After three 20 minutes long washing steps in 0.1 M phosphate buffer (PB) (pH 7.4) slices were fixated with 4% paraformaldehyde (PFA) in 0.2 M PB (pH 7.4) for 1 hour. Finally they were washed again three times in 0.1 M PB and stored at 4°C until staining was conducted within a few days.

2.4.2 Staining of fixated brain slices

The brain sections were washed once with 0.1 M PB and then incubated for 4 hours with the blocking solution containing 10% donkey serum (DKS), 2% bovine serum albumine (BSA) and 2% Triton X-100 in 0.1 M PB at room temperature. Microglia were visualized via an antibody directed against Ionized calcium-binding adapter molecule 1 (Iba1) (Wako). The antibody was diluted (1:600) in staining buffer containing 1% DKS, 0.2% BSA and 0.2% Triton X-100 in 0.1 M PB. Slices were incubated with the primary antibody overnight at room temperature.

To get rid of unbound antibodies slices were washed three times in 0.1 M PB for 20 minutes. To visualize the Iba1 expressing cells a secondary antibody directed against rabbit-Immunglobulin G (IgG) labeled with Alexa Fluor 647 was employed (Sigma-Aldrich). Slices were incubated with the secondary antibody diluted 1:250 in staining buffer for 2 hours at room temperature. They were washed again two times in 0.1 M PB and finally incubated for 15 minutes with 0.001% Thiazine Red R (Sigma-Aldrich) in 0.1 M PB to label the A β plaques. Slices were placed in 0.1 M PB for 10 minutes and mounted with Aqua-Poly/Mount (Polysciences) on glass slides.

2.4.3 Confocal laser scanning microscopy

Stainings were visualized using a Leica SPE Confocal Microscope. Phagocytic capabilities were assessed exclusively in the cortex of the slices, and only regions rich on beads were selected. Scans were done with a 10X objective, 1.5 zoom at a resolution of 1024x1024 pixel at a scan speed of 400 Hz. Z-stacks of 20 μm diameter in 1 μm steps starting from the top of the beads were made for all three channels, the BB microsphere (360→407 nm), Thiazine Red R (510→580 nm) and Alexa Fluor 647 (650→668 nm). Approximately 20 regions were scanned for each slice.

2.4.4 Data collection

The phagocytic index in the slices of the different mice was determined employing the Cell counter plugin by FIJI. Z-stacks were exported from the LEICA software as Tiff files and loaded in FIJI. The single images of every z-stack were transformed to a stack and the counted manually using the Cell Counter plugin to avoid double countings. Number of Iba1-positive cells as well as number of beads were recorded and registered in an Excel sheet. Scans belonging to the same individual were registered together and one phagocytic index for every mouse was calculated. Two different calculation methods were applied. A group analysis was conducted by calculating how many cells had phagocytosed 0, 1 to 4, 5 to 7, 8 to 10 or more than 10 beads. The percentage of cells for each group was multiplied with the factor 0, 1, 2, 3 or 4 respectively. The sum of it determined the phagocytic index for each z-stack. For the single analysis the percentage of cells having phagocytosed a certain number of beads was calculated, multiplied with this definite number and summarized. In both methods one phagocytic index for each mouse was calculated and averaged with those of mice with the same genotype and age.

2.5 Statistical analysis

Recorded data were analyzed using the SigmaStat 3.5 software (Systat Software). Only a minor part of the patch-clamp data were normally distributed, wherefore the Mann-Whitney rank-sum test was employed for all statistical tests. Data obtained from the phagocytosis assay were found to be normally distributed and

therefore a t-test was conducted. Test results were considered statistically significant and depicted according to the following scheme * $p=0.01-0.05$, ** $p=0.001-0.01$, *** $p<0.001$.

3. Results

3.1 Patch-clamp recordings

To assess the membrane properties of microglia in the cortex of 5XFAD mice over time animals at 1, 3 and 9 months of age were analyzed. Microglia were distinguished from other cells by their green fluorescence due to crossbreeding this mouse model with the MacGreen mouse. As controls, cortical microglia from offspring lacking the 5XFAD mutations were patched. It is known that microglial activation and density decreases with cell distance to A β plaques (Frautschy et al., 1998). Thus only A β plaque associated microglia were patched to assess the influences of A β peptides on microglial electrophysiology. In case of control and 1-month-old animals only randomly chosen microglia throughout the cortex were patched due to the lack of A β plaques in these animals. Membrane currents were recorded in whole-cell patch-clamp configuration after applying different voltage pulses in voltage clamp mode (see section 2.3.2). To compare current densities of microglia in acute slices whole-cell membrane currents were normalized to the membrane capacitance and the SEM were calculated.

3.1.1 Membrane properties of microglial cells

First the membrane properties of plaque-associated microglia in acute slices of 5XFAD and WT control mice at 1, 3 and 9 months of age were assessed. Membrane currents in microglia were evoked by a series of hyper- and depolarizing voltage steps ranging between -170 and 60 mV using a holding potential of -40 mV. Since the most negative and most positive voltage steps lead to the highest amplitudes, -170, -160 and -150 mV as well as 40, 50 and 60 mV were used to determine changes in membrane current density between different conditions.

3.1.1.1 Membrane current density in microglial cells of 5XFAD mice

A comparison of the inward current densities (Fig.4A) recorded at -170 , -160 and -150 mV in microglia of 5XFAD mice at 1 month (n=10) of age with those at 3

months (n=7) of age revealed a significant increase of inward rectifying K⁺ current densities in older mice (-170 mV: -3.706 ± 0.854 pA/pF vs. -35.375 ± 15.727 pA/pF, p=0.004; -160 mV: -3.699 ± 0.786 pA/pF vs. -33.633 ± 14.592 pA/pF, p=0.004; -150 mV: -3.563 ± 0.693 pA/pF vs. -31.152 ± 13.245 pA/pF, p=0.002). Inward rectifying current densities in microglia increased further when comparing 3 to 9 months (n=11) old TG animals (-170 mV: -35.375 ± 15.727 pA/pF vs. -82.717 ± 14.112 , p=0.019; -160 mV: -33.633 ± 14.592 pA/pF vs. -75.774 ± 142.204 pA/pF, p=0.019; -150 mV: -31.152 ± 13.245 pA/pF vs. -66.736 ± 10.494 pA/pF, p=0.024). In addition by comparing recordings of 1-month- and 9-month-old 5XFAD mice the differences in the measured membrane current densities were highly significant (-170 mV: -3.706 ± 0.854 pA/pF vs. -82.717 ± 14.112 pA/pF, p<0.001; -160 mV: -3.699 ± 0.786 pA/pF vs. -75.774 ± 142.204 pA/pF, p<0.001; -150 mV: -3.563 ± 0.693 pA/pF vs. -66.736 ± 10.494 pA/pF, p<0.001).

Regarding the outward rectifying current density (Fig. 4A) a significant increase in membrane current densities of microglia of 5XFAD mice between 1 month and 3 months of age at 40, 50 and 60 mV (40 mV: 1.733 ± 0.149 pA/pF vs. 5.295 ± 2.092 pA/pF, p=0.003; 50 mV: 2.020 ± 0.175 pA/pF vs. 6.316 ± 2.653 pA/pF, p=0.004; 60 mV: 2.334 ± 0.193 pA/pF vs. 7.344 ± 3.095 pA/pF, p=0.005) was detected. The current densities determined at 40, 50 and 60 mV in microglia of 5XFAD at 9 months of age were again elevated compared to mice at 3 months of age (40 mV: 19.706 ± 5.353 pA/pF vs. 5.295 ± 2.092 pA/pF, p=0.019; 50 mV: 22.430 ± 6.091 pA/pF vs. 6.316 ± 2.653 pA/pF, p=0.024; 60 mV: 25.375 ± 6.798 pA/pF vs. 7.344 ± 3.095 pA/pF, p=0.030). Outward membrane current densities evoked at 40, 50 and 60 mV in microglia of 9-month-old 5XFAD mice in contrast to 1-month-old animals were increased as well at a highly significant level (40 mV: 19.706 ± 5.353 pA/pF vs. 1.733 ± 0.149 pA/pF, p<0.001; 50 mV: 22.430 ± 6.091 pA/pF vs. 2.020 ± 0.175 pA/pF, p<0.001; 60 mV: 25.375 ± 6.798 pA/pF vs. 2.334 ± 0.193 pA/pF, p<0.001).

Altogether, these data demonstrate that microglia in the 5XFAD mouse model exhibit a steady increase in membrane current densities from 1 to 9 months of age.

3.1.1.2 Membrane current densities in microglial cells of WT mice

To check whether the change in membrane current density was due to age or a phenotype-related effect the current densities recorded in microglia in WT mice at

different ages (Fig.4B) were also tested. No significant differences in membrane current densities of microglia in WT mice at 1 month (n=5) and those at 3 months (n=19) of age at -170, -160 or -150 mV were observed (-170 mV: -3.700 ± 0.680 pA/pF vs. -4.946 ± 0.592 pA/pF, $p=0.570$; -160 mV: -3.698 ± 0.654 pA/pF vs. -4.967 ± 0.590 pA/pF, $p=0.477$; -150 mV: -3.773 ± 0.700 pA/pF vs. -4.813 ± 0.558 pA/pF; $p=0.522$). Comparing the membrane current densities measured in microglia of 3-month- and 9-month-old (n=15) WT animals showed no significant differences at the voltage steps between -170 mV and -150 mV (-170 mV: -4.946 ± 0.592 pA/pF vs. -7.044 ± 1.243 pA/pF, $p=0.103$; -160 mV: -4.967 ± 0.590 pA/pF vs. -6.849 ± 1.111 pA/pF, $p=0.083$; -150 mV: -4.813 ± 0.558 pA/pF vs. -6.516 ± 0.838 pA/pF, $p=0.066$). By comparing microglial membrane current densities after depolarizing voltage pulses from 1 month and 9 months old WT animals significant differences were only observed at -150 mV voltage steps (-170 mV: -3.700 ± 0.680 pA/pF vs. -7.044 ± 1.243 pA/pF, $p=0.081$; -160 mV: -3.698 ± 0.654 pA/pF vs. -6.849 ± 1.111 pA/pF, $p=0.055$; -150 mV: -3.773 ± 0.700 pA/pF vs. -6.516 ± 0.838 pA/pF; $p=0.045$).

Outward current densities in microglia of control mice (Fig.4B) were compared between 1 and 3 months of age at 40, 50 and 60 mV without any significant differences (40 mV: 1.960 ± 0.265 pA/pF vs. 1.722 ± 0.135 pA/pF, $p=0.355$; 50 mV: 2.318 ± 0.303 pA/pF vs. 2.057 ± 0.163 pA/pF, $p=0.320$; 60 mV: 2.623 ± 0.319 pA/pF vs. 2.453 ± 0.207 pA/pF, $p=0.570$). Moreover, the mean outward current densities measured in microglia at 40, 50 and 60 mV in WT mice at 3 months of age were not significantly different to those at 9 months of age (40 mV: 1.722 ± 0.135 pA/pF vs. 2.255 ± 0.231 pA/pF, $p=0.029$; 50 mV: 2.057 ± 0.163 pA/pF vs. 2.613 ± 0.279 pA/pF, $p=0.071$; 60 mV: 2.453 ± 0.207 pA/pF vs. 3.053 ± 0.366 pA/pF, $p=0.155$). Regarding the voltage pulses ranging from 40 to 60 mV no significant differences were found between WT mice at 1 month and 9 months of age (40 mV: 1.960 ± 0.265 pA/pF vs. 2.255 ± 0.231 pA/pF, $p=0.793$; 2.318 ± 0.303 pA/pF vs. 2.613 ± 0.279 pA/pF, $p=1.000$; 2.623 ± 0.319 pA/pF vs. 3.053 ± 0.366 pA/pF, $p=0.793$).

As a conclusion only minor age dependent differences were observed in microglial membrane properties of WT animals.

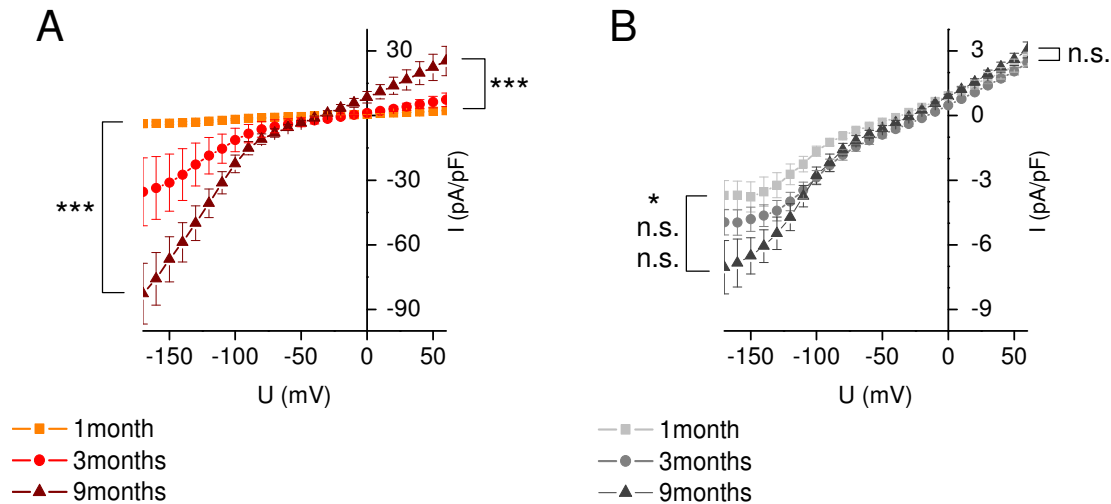


Fig.4. Age dependent membrane properties of microglial cells in 5XFAD and WT mice. Mean current densities (current normalized to the cell capacitance) of 5XFAD (A) and WT (B) mice at 1, 3 and 9 months of age. Membrane currents were recorded in response to voltage steps ranging from -170 to 60 mV lasting for 50 ms using a holding potential of -40 mV. Data are given as mean \pm SEM. Note the different scaling. Significance levels between 1 and 9 months of age at -170, -160 and -140 mV are indicated left to each graph and those at 40, 50 and 60 mV right to each graph . * $p=0.01-0.05$, ** $p=0.001-0.01$, *** $p<0.001$. Note that the only significant difference between WT mice of 1 and 9 months of age were measured at -150 mV.

3.1.1.2 Comparison of membrane properties of microglial cells in age matched 5XFAD and WT mice

The resting membrane potential (RMP) for microglia in 5XFAD and WT mice at 1 month age of was determined to be -35.201 ± 4.713 mV and -35.917 ± 2.566 mV on average. The mean membrane current densities recorded in microglia of 5XFAD mice (n=10) at -170, -160 and -150 mV resulted in mean inward rectifying current densities, which were similar to those in WT mice (n=5)(Fig. 5D) (-170 mV: -3.706 ± 0.854 pA/pF vs. -3.700 ± 0.680 pA/pF, $p=0.582$; -160 mV: -3.669 ± 0.786 pA/pF vs. -3.698 ± 0.654 pA/pF, $p=0.501$; -150 mV: -3.563 ± 0.693 pA/pF vs. 3.773 ± 0.700 pA/pF, $p=0.501$). No significant differences between the two groups at positive potentials of 40, 50 and 60 mV were measured. (40 mV: 1.733 ± 0.149 pA/pF vs. 1.960 ± 0.265 pA/pF, $p=0.582$; 50 mV: 2.020 ± 0.175 pA/pF vs. 2.318 ± 0.303 pA/pF, $p=0.582$; 60 mV: 2.334 ± 0.193 pA/pF vs. 2.623 ± 0.319 pA/pF, $p=0.668$). In summary, there was no increment neither

of inward nor of outward current densities in microglia found in slices of 1-month-old TG mice in comparison to WT controls (Fig.5D)

Microglia of 5XFAD (n=19) and WT mice (n=7) at 3 months of age had average RMP's of -22.409 ± 5.554 mV and -27.240 ± 2.155 mV respectively. The mean microglial membrane current densities recorded in acute slices of 5XFAD and WT animals at 3 months of age (Fig. 5E) were found to be significantly different from each other at the voltage pulses between -170 mV to -150 mV (-170 mV: -35.375 ± 15.727 pA/pF vs. -4.946 ± 0.592 pA/pF, $p=0.005$; -160 mV: -33.633 ± 14.592 pA/pF vs. -4.976 ± 0.590 pA/pF, $p=0.004$; -150 mV: -31.152 ± 13.245 pA/pF vs. -4.813 ± 0.558 pA/pF, $p=0.002$). In addition membrane current densities of microglia in 5XFAD mice were significantly increased in comparison to those in WT animals (40 mV: 5.295 ± 2.092 pA/pF vs. 1.722 ± 0.135 pA/pF, $p=0.002$; 50 mV: 6.316 ± 2.653 pA/pF vs. 2.057 ± 0.163 pA/pF, $p=0.003$; 60 mV: 7.344 ± 3.095 pA/pF vs. 2.453 ± 0.207 pA/pF, $p=0.006$). Hence, microglia in and around A β plaques of 3-month-old 5XFAD mice exhibit on average a significantly increased inward rectifying current density in contrast to their WT controls (Fig.5E). Moreover also the mean outward current densities were found to be significantly increased in A β plaque-associated microglia of 5XFAD animals in comparison to the age-matched control mice, although to a lesser extent than the inward current densities. Note the different scaling in comparison to the 1-month-old mice.

At 9 months of age the resting membrane potential of 5XFAD (n=11) and WT (n=15) mice was -33.867 ± 4.557 mV and -30.513 ± 2.472 mV, respectively. Microglia patched in cortical A β plaques of 5XFAD mice demonstrated again enhanced membrane current densities ranging from -82.717 ± 14.112 pA/pF at voltages of -170 mV to 25.375 ± 6.798 pA/pF at 60 mV (Fig. 5F). Microglia in 5XFAD mice exposed to the three most negative voltage pulses, namely -170, -160 and -150 mV showed significantly increased mean membrane current densities compared to their controls (-170 mV: -82.717 ± 14.122 pA/pF vs. -7.044 ± 1.243 pA/pF, $p<0.001$; -160 mV: -75.774 ± 12.204 pA/pF vs. -6.849 ± 1.111 pA/pF, $p<0.001$; -150 mV: -66.736 ± 10.494 pA/pF vs. -6.516 ± 0.838 pA/pF, $p<0.001$). Voltage pulses between 40 and 60 mV elicited significantly elevated membrane .in microglia of 5XFAD mice in contrast to WT animals (40 mV: 19.706 ± 5.353 pA/pF vs. 2.255 ± 0.231 pA/pF, $p<0.001$; 50 mV: 22.430 ± 6.091

pA/pF vs. 2.613 ± 0.279 pA/pF, $p < 0.001$; 60 mV: 25.375 ± 6.798 pA/pF vs. 3.053 ± 0.366 pA/pF, $p < 0.001$).

Thus the present data display that both, inward and outward current is significantly increased in 5XFAD mice at 3 and 9 months of age when compared to age-matched controls. However, there were no differences at 1 month of age.

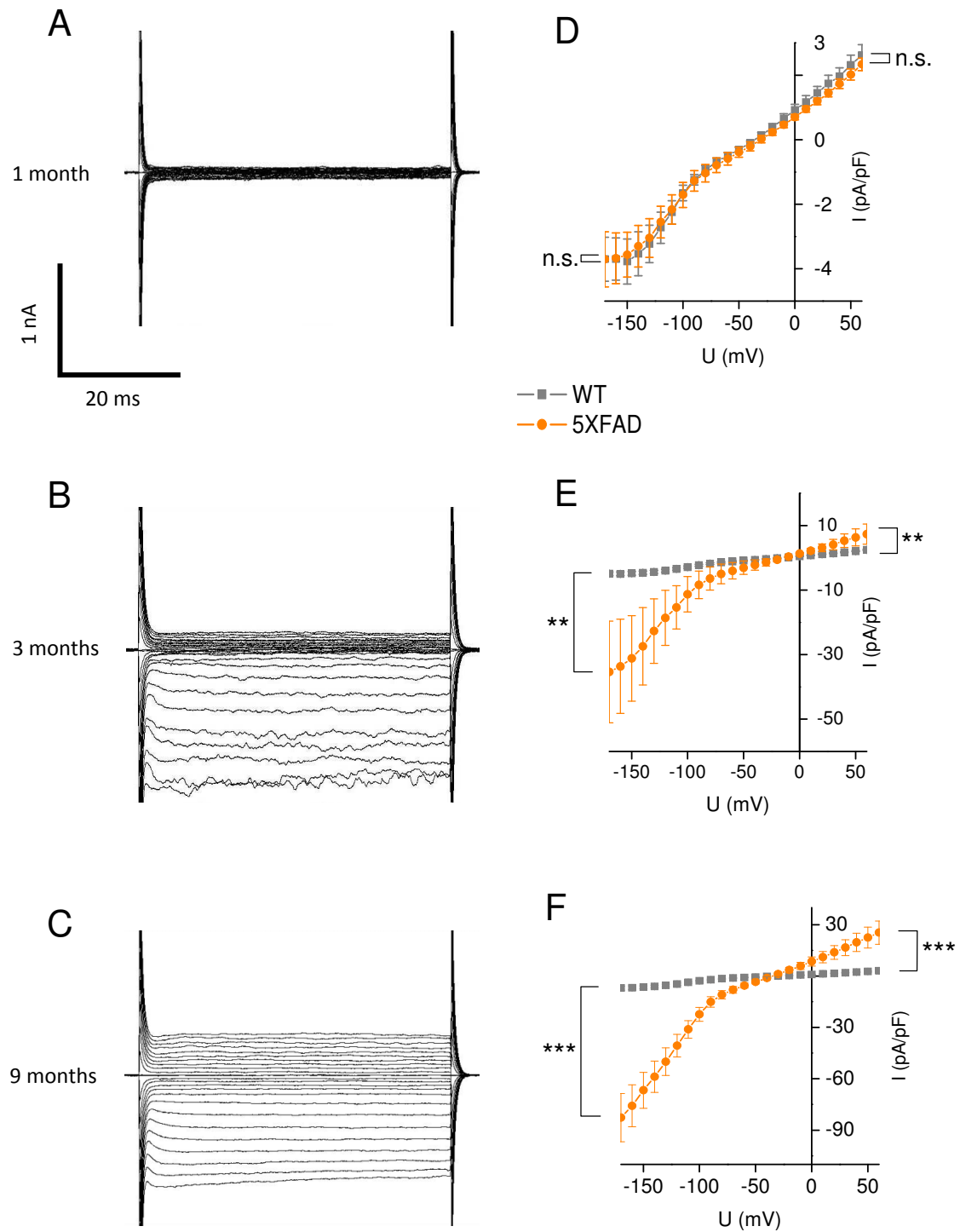


Fig. 5. Microglial membrane currents of 5XFAD and WT mice in direct comparison. Data were acquired in response to voltage steps ranging from -170 to 60 mV lasting for 50 ms using a holding potential of -40 mV. Example recordings of microglia in 5XFAD mice at 1, 3 and 9 months of age (A, B, C). Mean current density (current normalized to the cell capacitance) of microglia in acute slices of 5XFAD and WT mice at 1, 3 and 9 months of age (D, E, F). Data are given as mean \pm SEM. Significance levels between TG and WT mice at -170, -160 and -140 mV are indicated left to each graph and those at 40, 50 and 60 mV right to each graph. * $p=0.01-0.05$, ** $p=0.001-0.01$, *** $p<0.001$.

Altogether these data demonstrate that microglia in 5XFAD mice exhibit a statistically significant increase in their membrane current densities between 1 and 9 months of age, while changes in membrane current densities were practically absent in microglia of WT controls. Moreover the membrane current densities displayed at 3 and 9 months of age by microglia of 5XFAD mice were significantly higher than in age-matched WT animals.

3.1.2 Purinergic receptor agonist induced currents

It is well established that microglia express a variety of receptors on their surface, amongst others purinergic receptors. The expression of the P2X7 receptor is related to a variety of brain pathologies (Monif et al., 2010) and its upregulation especially in microglia of an AD mouse model was linked to neuronal damage (Lee et al., 2010). Therefore possible alterations in the responsiveness of plaque-associated microglia in the cortex of 5XFAD mice to the activation of purinergic receptors were investigated. During 10-minute recordings of a series of de- and hyperpolarizing steps, ATP (1 mM) and BzATP (0,15 mM) were applied to the bath solution. (see section 2.3.2) The ACSF used was free of divalent cations to elicit bigger current responses (Boucsein, 2003).

3.1.2.1 Differences in purinergic current responses at different ages

To test whether ATP responses in microglia of 5XFAD and WT mice did depend on age the mean currents flowing at -140, -120 and 100 mV, as well as at 20, 40 and 60 mV were compared between the different age groups for 5XFAD and WT mice separately.

3.1.2.1.1 ATP responses at different ages in 5XFAD and WT mice

In contrast to microglia in 1-month-old 5XFAD mice (n=5) the cells in 3-month-old ones (n=10) exhibited significantly smaller mean inward currents at -140, -120 and -100 mV (-140 mV: -1.072 ± 0.274 nA vs. -0.316 ± 0.065 nA, $p=0.013$; -120 mV: -0.889 ± 0.222 nA vs. -0.256 ± 0.051 nA, $p=0.007$; -100 mV: -0.712 ± 0.171 nA vs. -0.206 ± 0.042 nA, $p=0.007$) (Fig.6A). Moreover also outward currents elicited by 20, 40 and 60 mV in 3-month-old TG mice were significantly reduced in relation to 1-month-old mice (20 mV: 0.026 ± 0.006 nA vs. 0.122 ± 0.028 nA, $p=0.005$; 40 mV: 0.053 ± 0.012 nA vs. 0.233 ± 0.051 nA, $p=0.005$; 60 mV: 0.078 ± 0.017 nA vs. 0.340 ± 0.077 nA, $p=0.007$). Mean microglial currents recorded at -140, -120 and -100 mV in 5XFAD at 9 months of age (n=5) were again smaller than at 3 months of age (Fig.6A), but this difference did not reach significance (-140 mV: -0.180 ± 0.084 nA vs. -0.316 ± 0.065 nA, $p=0.213$; -120 mV: -0.152 ± 0.062 nA vs. -0.256 ± 0.051 nA, $p=0.257$; -100 mV: -0.129 ± 0.044 nA vs. -0.206 ± 0.042 nA, $p=0.257$). However, the membrane currents evoked at 20, 40 and 60 mV in 9-month-old 5XFAD were significantly reduced in contrast to 3-month-old mice (20 mV: -0.005 ± 0.011 vs. 0.026 ± 0.006 , $p=0.009$; 40 mV: -0.002 ± 0.015 vs. 0.053 ± 0.012 , $p=0.009$; 60 mV: 0.007 ± 0.018 vs. 0.078 ± 0.017 , $p=0.023$). By comparing the ATP-evoked currents expressed by microglia at the three most negative voltage pulses in 5XFAD at 1 month and at 9 months of age significant differences were detected (-140 mV: -1.072 ± 0.274 nA vs. -0.180 ± 0.084 nA, $p=0.016$; -120 mV: -0.889 ± 0.222 nA vs. -0.152 ± 0.062 nA, $p=0.016$; -100 mV: -0.712 ± 0.171 nA vs. -0.129 ± 0.044 nA, $p=0.016$) (Fig.6A). Moreover, the microglial membrane currents at the three most positive voltage pulses demonstrated significantly reduced amplitudes upon ATP exposure in 9-month-old 5XFAD in contrast to 1-month-old mice (20 mV: -0.005 ± 0.011 nA vs. 0.122 ± 0.028 nA, $p=0.008$; 40 mV: -0.002 ± 0.015 nA vs. 0.233 ± 0.051 nA, $p=0.008$; 60 mV: 0.007 ± 0.018 nA vs. 0.340 ± 0.077 nA, $p=0.008$).

Next, membrane currents in response to ATP in microglia of acute slices prepared from WT mice at 1, 3, and 9 months of age were analyzed. While a similar decrease in mean membrane current upon activation of purinergic receptors in microglia of 5XFAD mice was detected in those of WT mice, the differences found at -

140, -120 and -100 mV in 1-month- (n=5) and 3-month-old mice (n=14) were not significant (-140 mV: -0.754 ± 0.355 nA vs. -0.434 ± 0.065 nA, $p=0.087$; -120 mV: -0.630 ± 0.306 nA vs. -0.334 ± 0.051 nA, $p=0.087$; -100 mV: -0.504 ± 0.245 nA vs. -0.254 ± 0.040 nA, $p=0.087$) (Fig.6B). In accordance to this no significant differences in microglial ATP-activated membrane currents between 1 month and 3-month-old WT mice were found at voltages between 20 and 60 mV (20 mV: -0.077 ± 0.041 nA vs. 0.030 ± 0.005 nA, $p=0.127$; 40 mV: -0.153 ± 0.077 nA vs. 0.061 ± 0.011 nA, $p=0.105$; 60 mV: 0.224 ± 0.112 nA vs. 0.061 ± 0.017 nA, $p=0.105$). Comparing the membrane currents displayed by microglia in WT animals at 3 and 9 months of age (n=10) (Fig.6B) no significant differences were detected at -140, -120 and -100 mV (-140 mV: -0.434 ± 0.065 nA vs. -0.320 ± 0.087 nA, $p=0.151$; -120 mV: -0.334 ± 0.051 nA vs. -0.242 ± 0.068 nA, $p=0.121$; -100 mV: -0.254 ± 0.040 nA vs. -0.186 ± 0.053 nA, $p=0.151$). Also ATP-evoked currents in microglia of 3-month- and 9-month-old mice at 20, 40 and 60 mV yielded no significant differences (20 mV: 0.030 ± 0.005 nA vs. 0.023 ± 0.008 nA, $p=0.306$; 40 mV: 0.061 ± 0.011 nA vs. 0.046 ± 0.015 nA, $p=0.188$; 60 mV: 0.061 ± 0.017 nA vs. 0.070 ± 0.022 , $p=0.230$). Comparing currents recorded in microglia of 1-month- and 9-month-old WT animals at depolarizing voltages upon ATP application (Fig.6B) showed that they were not significantly different from each other (-140 mV: -0.754 ± 0.355 nA vs. -0.320 ± 0.087 nA, $p=0.098$; -120 mV: -0.630 ± 0.306 nA vs. -0.242 ± 0.068 nA, $p=0.076$; -100 mV: -0.504 ± 0.245 nA vs. -0.186 ± 0.053 nA, $p=0.098$). Microglia in WT mice at 1 month of age and at 9 month of age did not differ in their outward currents to be significantly different (20 mV: -0.077 ± 0.041 nA vs. 0.023 ± 0.008 nA, $p=0.126$; 40 mV: -0.153 ± 0.077 nA vs. 0.046 ± 0.015 nA, $p=0.098$; 60 mV: 0.224 ± 0.112 nA vs. 0.070 ± 0.022 nA, $p=0.098$).

Taken together, these data show that microglia in the 5XFAD mouse exhibit a decrease in responsiveness to ATP with age, which cannot be found in WT mice (Fig.6A/6B).

3.1.2.1.2 BzATP responses at different ages in 5XFAD and WT mice

Age-related alterations in P2X7-specific responsiveness of microglia were assessed by comparing the membrane currents recorded after BzATP application at different ages for 5XFAD and WT mice separately. Although microglia in 3-month-old

5XFAD (n=13) exhibited smaller outward currents at -140, -120 and -100 mV than 1-month-old animals (n=5) (Fig.6C), these differences were not significant (-140 mV: -0.475 ± 0.137 nA vs. -0.976 ± 0.272 nA, $p=0.168$; -120 mV: -0.805 ± 0.228 nA vs. -0.526 ± 0.071 nA, $p=0.115$; -100 mV: -0.304 ± 0.093 vs. -0.645 ± 0.190 nA, $p=0.139$). Also the outward currents of microglia in 1-month- and 3-month-old mice yielded no significant results (20 mV: 0.103 ± 0.031 nA vs. 0.044 ± 0.019 nA, $p=0.237$; 40 mV: 0.198 ± 0.062 nA vs. 0.087 ± 0.034 nA, $p=0.200$; 60 mV: 0.293 ± 0.091 nA vs. 0.128 ± 0.050 nA, $p=0.200$). When BzATP evoked currents of microglia in 3-month-old 5XFAD were compared to those in 9-month-old animals (n=7) a further decrease in ion currents was detected with age (Fig. 6C), but this was not significant for -140, -120 and -100 mV (-140 mV: -0.475 ± 0.137 nA vs. -0.266 ± 0.094 nA, $p=0.178$; -120 mV: -0.381 ± 0.115 nA vs. -0.226 ± 0.071 nA, $p=0.303$; -100 mV: -0.304 ± 0.093 vs. -0.181 ± 0.056 nA, $p=0.235$). Comparing the microglial responses at 20, 40 and 60 mV revealed a significantly lower current in microglia of 9-month- than in 3-month-old TG mice (20 mV: -0.004 ± 0.012 nA vs. 0.044 ± 0.019 nA, $p=0.027$; 40 mV: 0.007 ± 0.016 nA vs. 0.087 ± 0.034 nA, $p=0.032$; 60 mV: 0.019 ± 0.020 nA vs. 0.128 ± 0.050 nA, $p=0.048$). When BzATP-elicited membrane currents in microglia of 5XFAD at 1 month of age were compared with those at 9 months of age (Fig.6C) differences were significant only at -140 and -120 mV (-140 mV: -0.976 ± 0.272 nA vs. -0.266 ± 0.094 nA, $p=0.030$; -120 mV: -0.805 ± 0.228 nA vs. -0.226 ± 0.071 nA, $p=0.048$; -100 mV: -0.645 ± 0.190 nA vs. -0.181 ± 0.056 nA, $p=0.073$). Also the microglial membrane currents triggered by BzATP at 20, 40 and 60 mV were significantly different between mice at 1 month of age and those at 9 months of age (20 mV: 0.103 ± 0.031 nA vs. -0.004 ± 0.012 nA, $p=0.030$; 40 mV: 0.198 ± 0.062 nA vs. -0.007 ± 0.016 nA, $p=0.048$; 60 mV: 0.293 ± 0.091 nA vs. -0.019 ± 0.020 nA, $p=0.048$).

Regarding the membrane currents in microglia of WT animals upon BzATP application, no significant differences between mice at 1 month (n=5) and 3 months of age (n=17) (Fig.6D) were found at -140, -120 and -100 mV (-140 mV: -0.915 ± 0.252 nA vs. -0.653 ± 0.084 nA, $p=0.308$; -120 mV: -0.740 ± 0.270 nA vs. -0.526 ± 0.071 nA, $p=0.308$; -100 mV: -0.587 ± 0.168 nA vs. -0.411 ± 0.057 nA, $p=0.308$). Although larger mean currents at 20, 40 and 60 mV were detected in microglia of younger mice, no significant differences were reached when data of 1-month- and 3-month-old mice

were compared (20 mV: 0.074 ± 0.025 nA vs. 0.057 ± 0.010 nA, $p=0.481$; 40 mV: 0.150 ± 0.049 nA vs. 0.115 ± 0.019 nA, $p=0.531$; 60 mV: 0.227 ± 0.072 nA vs. 0.170 ± 0.028 nA, $p=0.481$). 9-month-old WT mice ($n=11$) exhibited significantly decreased inward currents in contrast to those of 3-month-old animals (-140 mV: -0.653 ± 0.084 nA vs. -0.330 ± 0.143 nA, $p=0.008$; -120 mV: -0.526 ± 0.071 nA vs. -0.263 ± 0.116 nA, $p=0.007$; -100 mV: -0.411 ± 0.057 nA vs. -0.210 ± 0.093 nA, $p=0.008$) (Fig.6D). Also the membrane currents measured in WT microglia at depolarizing voltage pulses were significantly smaller at 9 months than at 3 months of age (20 mV: 0.025 ± 0.013 nA vs. 0.057 ± 0.010 nA, $p=0.007$; 40 mV: 0.001 ± 0.025 nA vs. 0.115 ± 0.019 nA, $p=0.010$; 60 mV: 0.170 ± 0.028 nA, $p=0.010$). Surprisingly, the decrease in microglial membrane currents upon BzATP application from 1 to 9 months of age in WT animals (Fig.6D) was statistically not significant neither at the most negative voltage steps (-140 mV: -0.915 ± 0.252 nA vs. -0.330 ± 0.143 nA, $p=0.089$; -120 mV: -0.740 ± 0.270 nA vs. -0.236 ± 0.116 nA, $p=0.089$; -100 mV: -0.587 ± 0.168 nA vs. -0.210 ± 0.093 nA, $p=0.089$), nor at the most positive voltages measured (20 mV: 0.074 ± 0.025 nA vs. 0.025 ± 0.013 nA, $p=0.213$; 40 mV: 0.150 ± 0.049 nA vs. 0.050 ± 0.025 nA, $p=0.141$; 60 mV: 0.227 ± 0.072 nA vs. 0.076 ± 0.036 nA, $p=0.141$).

The present data demonstrate a significant decrease in purinergic responsiveness in 5XFAD mice from 1 to 9 months of age. This effect was more pronounced for ATP than BzATP, which acts only on the P2X7 receptor. Although a similar trend was detected in microglia of WT mice, data were not significantly different. However, a significant decrease in membrane currents was spotted in WT mice between 3 and 9 months of age.

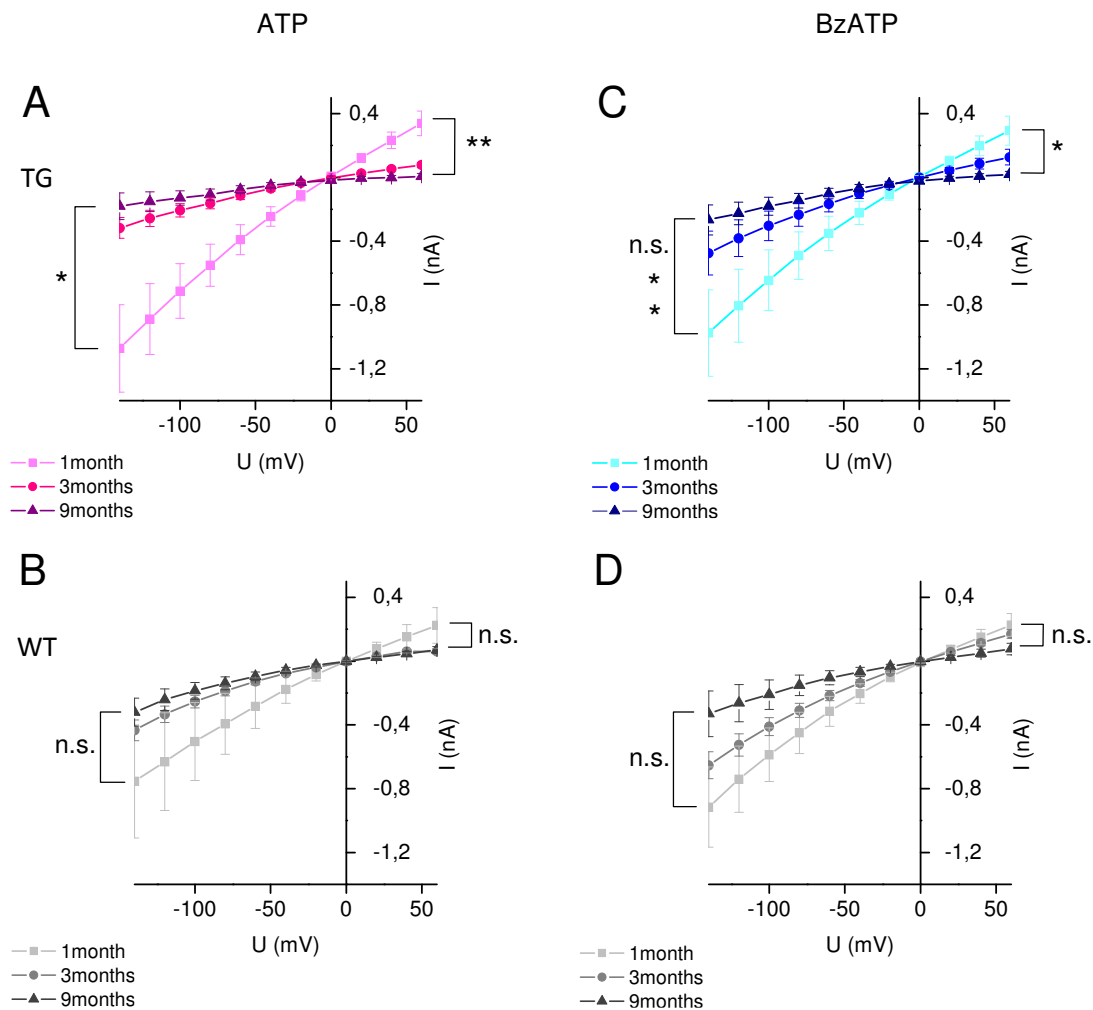


Fig.6. Electrophysiological responses of microglia exposed to ATP (A, B) and BzATP (C, D). Current-voltage curves were recorded from microglia of the 5XFAD mouse model (A, C) and WT control mice (B, D) at 1, 3 and 9 months of age. Membrane currents at different voltages were gained from recordings, during which the cells were subsequently de- and hyperpolarized by applying a series of voltage steps ranging from -140 mV to 60 mV. Recordings were obtained while cells were perfused with Ca^{2+}/Mg^{2+} -free ACSF. Data are given as mean \pm SEM. Significance levels between 1 and 9 months of age at -140, -120 and -100 mV are indicated left to each graph and those at 20, 40 and 60 mV right to each graph. * $p=0.01-0.05$, ** $p=0.001-0.01$, *** $p<0.001$.

3.1.2.1 Differences in purinergic responses between 5XFAD and WT mice

ATP evoked a membrane current increase in microglia of both, 5XFAD and WT mice at 1, 3 and 9 months of age.

Although the inward current elicited by this substance was slightly bigger in cells from acute slices of the 5XFAD mouse than in controls (Fig.7A) the analysis of the mean currents evoked at -140 mV, -120 mV and -100 mV in microglia of TG and WT

mice at 1 months of age did not reach significance for ATP (-140 mV: -1.072 ± 0.274 nA vs. -0.754 ± 0.355 nA, $p=0.310$; -120 mV: -0.889 ± 0.222 nA vs. -0.630 ± 0.306 nA, $p=0.412$; -100 mV: -0.712 ± 0.171 nA vs. -0.504 ± 0.245 nA, $p=0.412$). Similar to the inward current, the outward currents recorded in microglia of 1-month-old TG mice at 20, 40 and 60 mV were comparable to age-matched controls (0.122 ± 0.028 nA vs. -0.077 ± 0.041 nA, $p=0.310$; 0.233 ± 0.051 nA vs. -0.153 ± 0.077 nA, $p=0.310$; 0.340 ± 0.077 nA vs. 0.224 ± 0.112 nA, $p=0.310$). Regarding the inward currents elicited by ATP in microglia of 3-month-old TG and control mice (Fig.7B) yielded no significant differences (-140 mV: -0.316 ± 0.065 nA vs. -0.434 ± 0.065 nA, $p=0.218$; -120 mV: -0.256 ± 0.051 nA vs. -0.334 ± 0.051 nA, $p=0.286$; -100 mV: -0.206 ± 0.042 nA vs. -0.254 ± 0.040 nA, $p=0.366$). ATP-activated currents recorded at 20, 40 and 60 mV of TG mice at 3 months of age were also similar to WT levels (20 mV: 0.026 ± 0.006 nA vs. 0.030 ± 0.005 nA, $p=0.565$; 40 mV: 0.053 ± 0.012 nA vs. 0.061 ± 0.011 nA, $p=0.681$; 60 mV: 0.078 ± 0.017 nA vs. 0.061 ± 0.017 nA, $p=0.529$). This pattern was repeated when ATP-activated currents at -140, -120 and -100 mV recorded in microglia of 9-month-old 5XFAD were compared with those in age-matched WT controls (-140 mV: -0.180 ± 0.084 nA vs. -0.320 ± 0.087 nA, $p=0.298$; -120 mV: -0.152 ± 0.062 nA vs. -0.242 ± 0.068 nA, $p=0.426$; -100 mV: -0.129 ± 0.044 nA vs. -0.186 ± 0.053 nA, $p=0.759$) (Fig.7C). Currents recorded in microglia at 20, 40 and 60 mV upon ATP application were not entirely outward directed in 9-month-old animals, but similar in amplitude between 5XFAD and WT mice (20 mV: -0.005 ± 0.011 vs. 0.023 ± 0.008 , $p=0.076$; 40 mV: -0.002 ± 0.015 vs. 0.046 ± 0.015 , $p=0.159$; 60 mV: 0.007 ± 0.018 vs. 0.070 ± 0.022 , $p=0.058$).

Since P2X7 was shown to be upregulated in disease condition, P2X7-specific alterations in microglial purinergic responsiveness in 5XFAD in contrast to WT controls were investigated. The P2X7-specific agonist BzATP triggered comparable responses in microglia of 5XFAD and WT mice at 1 months of age (Fig.7D) at -140, -120 and -100 mV (-140 mV: -0.976 ± 0.272 nA vs. -0.915 ± 0.252 nA, $p=0.690$; -120 mV: -0.805 ± 0.228 nA vs. -0.740 ± 0.207 nA, $p=0.690$; -100 mV: -0.645 ± 0.190 nA vs. -0.587 ± 0.168 nA, $p=0.690$). Regarding the currents evoked at 20, 40 and 60 mV in response BzATP microglia of 5XFAD and WT mice at 1 month of age showed no significant difference (20 mV: 0.103 ± 0.031 nA vs. 0.074 ± 0.025 nA, $p=0.548$; 40 mV: 0.198 ± 0.062 nA vs. 0.150 ± 0.049 nA, $p=0.690$; 60 mV: 0.293 ± 0.091 nA vs. 0.227 ± 0.072 nA, $p=0.548$).

The three most negative voltage steps during BzATP application yielded significant differences in inward currents between microglia of 3-month-old 5XFAD and age-matched-controls (Fig.7E) only at -100 mV (-140 mV: -0.475 ± 0.137 nA vs. -0.653 ± 0.084 nA, $p=0.066$; -120 mV: -0.381 ± 0.115 nA vs. -0.526 ± 0.071 nA, $p=0.054$; -100 mV: -0.304 ± 0.093 vs. -0.411 ± 0.057 nA, $p=0.049$). At 3 months of age significant differences in BzATP activated currents recorded in microglia at 20, 40 and 60 mV between TG and WT mice were only detected at the 20 mV pulse (20 mV: 0.044 ± 0.019 nA vs. 0.057 ± 0.010 nA, $p=0.04$; 40 mV: 0.087 ± 0.034 nA vs. 0.115 ± 0.019 nA, $p=0.079$; 60 mV: 0.128 ± 0.050 nA vs. 0.170 ± 0.028 nA, $p=0.079$). BzATP evoked currents at -140, -120 and -100 mV recorded in microglia of 9-month-old 5XFAD were compared with those in age-matched WT controls (Fig.7F) revealing no significant differences (-140 mV: -0.266 ± 0.094 nA vs. -0.330 ± 0.143 nA, $p=0.786$; -120 mV: -0.226 ± 0.071 nA vs. -0.263 ± 0.116 nA, $p=0.469$; -100 mV: -0.181 ± 0.056 nA vs. -0.210 ± 0.093 nA, $p=0.319$). In microglia of 9-month-old 5XFAD mice the mean BzATP responses assessed at 20, 40 and 60 mV were found to be not significantly different from those in WT animals at the same age (20 mV: -0.004 ± 0.012 nA vs. 0.025 ± 0.013 nA, $p=0.277$; 40 mV: 0.007 ± 0.016 nA vs. 0.050 ± 0.025 nA, $p=0.239$; 60 mV: 0.019 ± 0.020 nA vs. 0.076 ± 0.036 nA, $p=0.365$).

In summary, no significant differences between 5XFAD and WT animals in microglial membrane currents in response to ATP or BzATP was detected. This finding was true at 1, 3 and 9 months of age suggesting that purinergic signaling is relatively unmodified in the AD mouse model.

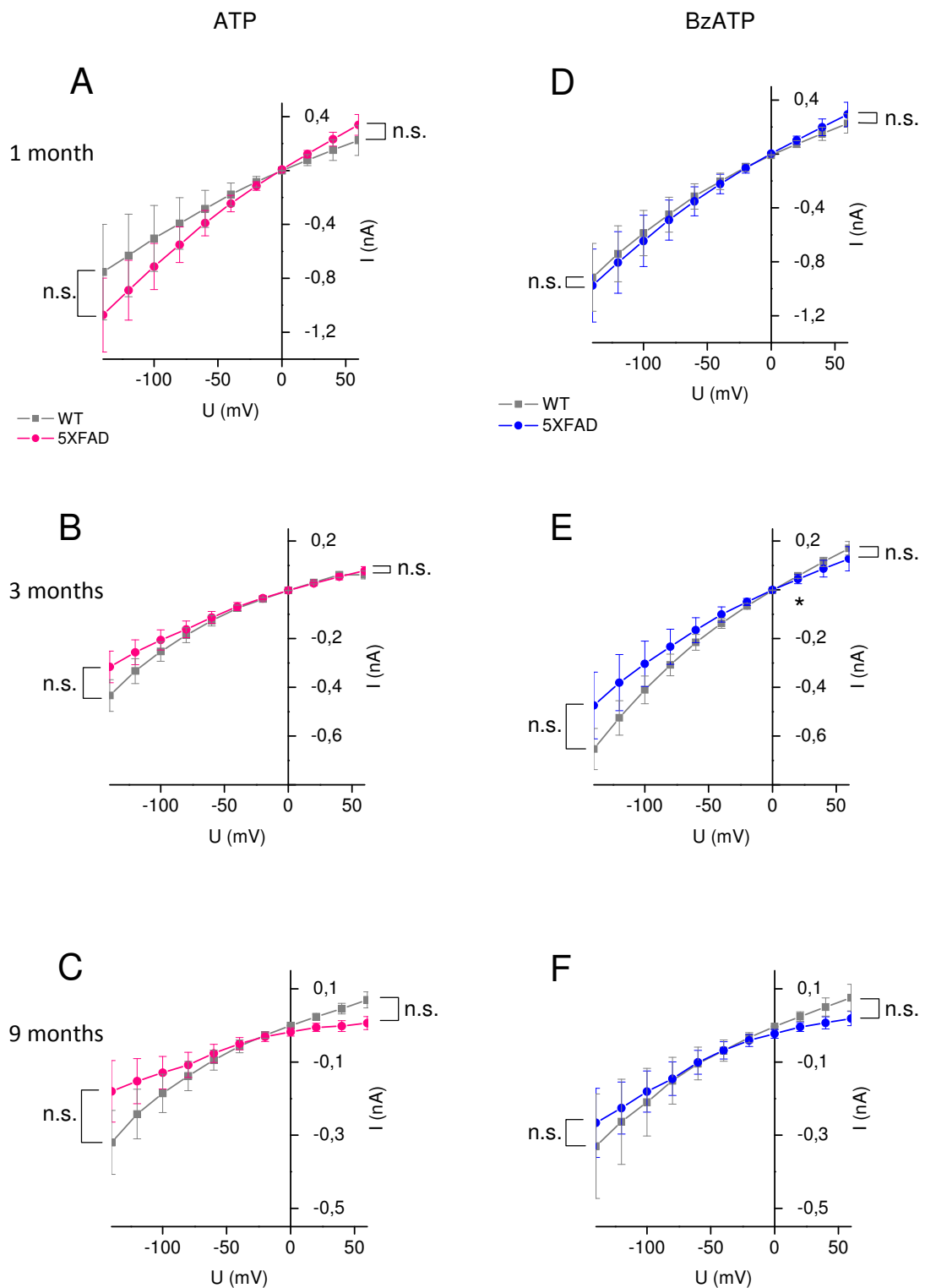


Fig.7. Responses of microglia to ATP and the P2X7-specific agonist BzATP in acute slice of 5XFAD mice and WT controls at 1 (A, D), 3 (B, E) and 9 (C, F) months of age. The current-voltage curves were gained from recordings marked by de- and hyperpolarizing voltage steps in the range of -140 mV to 60 mV lasting for 100 ms at a holding potential of -40 mV. Cells were constantly perfused with $\text{Ca}^{2+}/\text{Mg}^{2+}$ -free ACSF. Data are given as mean \pm SEM. Significance levels between 1 and 9 months of age at -140, -120

and -100 mV are indicated left to each graph and those at 20, 40 and 60 mV right to each graph. * $p=0.01-0.05$, ** $p=0.001-0.01$, *** $p<0.001$.

3.2 Phagocytosis in microglia of 9-month-old 5XFAD mice is reduced

Microglia are known to perform phagocytosis of pathogens, of cell debris but also of A β peptide. Impairment of phagocytic capacity in microglia is well documented for other AD mouse models (Krabbe et al., 2013) but not for the present one. Since the 5XFAD mouse is phenotypically marked by an especially fast accumulation of A β plaques it was of great importance to assess whether microglia in this mouse model demonstrate an altered readiness to phagocytic activity. Therefore a phagocytosis assay with FBS-coated fluorescent microspheres was carried out (see section 2.4) with acute brain slices from 9 month old 5XFAD (n=3) and age-matched WT mice (n=3).

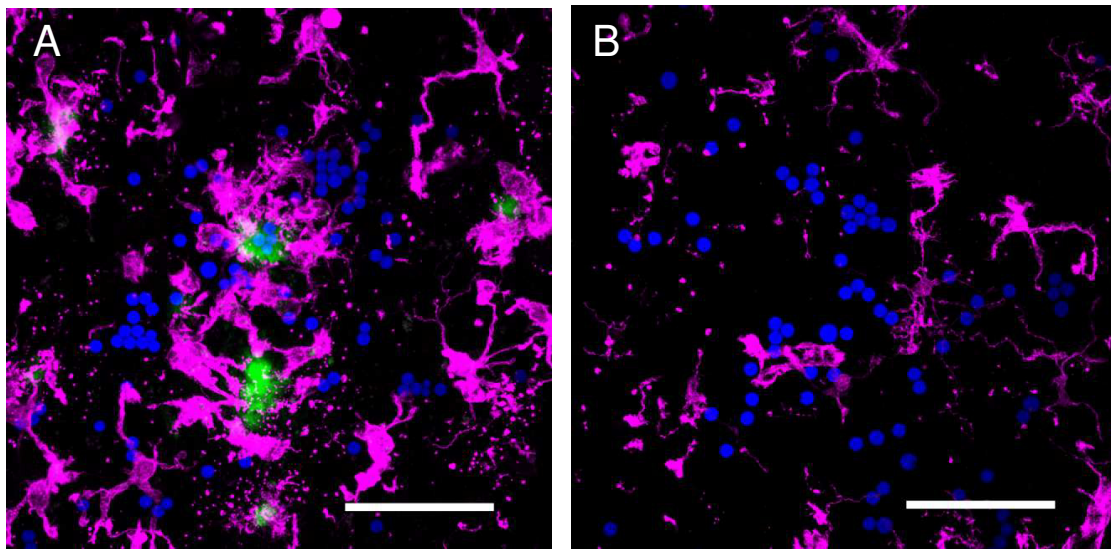


Fig.8. Representative Z-projections of 20 μm thick confocal scans from a 5XFAD (A) and a WT (B) mouse. Microglia are depicted in magenta, microspheres in blue and dense core plaques in green. Scale bars: 50 μm .

Already the z-stacks from stained brain slices revealed a very distinct phenotype of microglia in the 5XFAD brain (Fig.8A). They outnumbered by far the number of cells seen in the controls and clustered in the form of rosettes around A β depositions stained with Thiazine red. Microglia directly associated with A β plaques exhibited an amoeboid shape and sometimes a Thiazine red R signal was detectable

40

even in their soma. In contrast to this microglia stained in WT animals (Fig.8B) were regularly fewer in number and evenly distributed in the scanned areas.

The group analysis clearly showed that the microglia in acute brain slices of the 5XFAD mouse model phagocytosed significantly less beads during 1 hour of incubation than the same cell type in sections from WT controls (Fig.9A) represented by the phagocytic index (14.085 ± 1.750 arbitrary units (a.u.) vs. 26.174 ± 1.937 a.u., $p=0.012$). This difference was even more distinct in the single analysis (Fig.9B) when every phagocytosed bead was entered in the calculation separately (17.116 ± 2.516 a.u. vs. 32.356 ± 1.786 a.u., $p=0.005$).

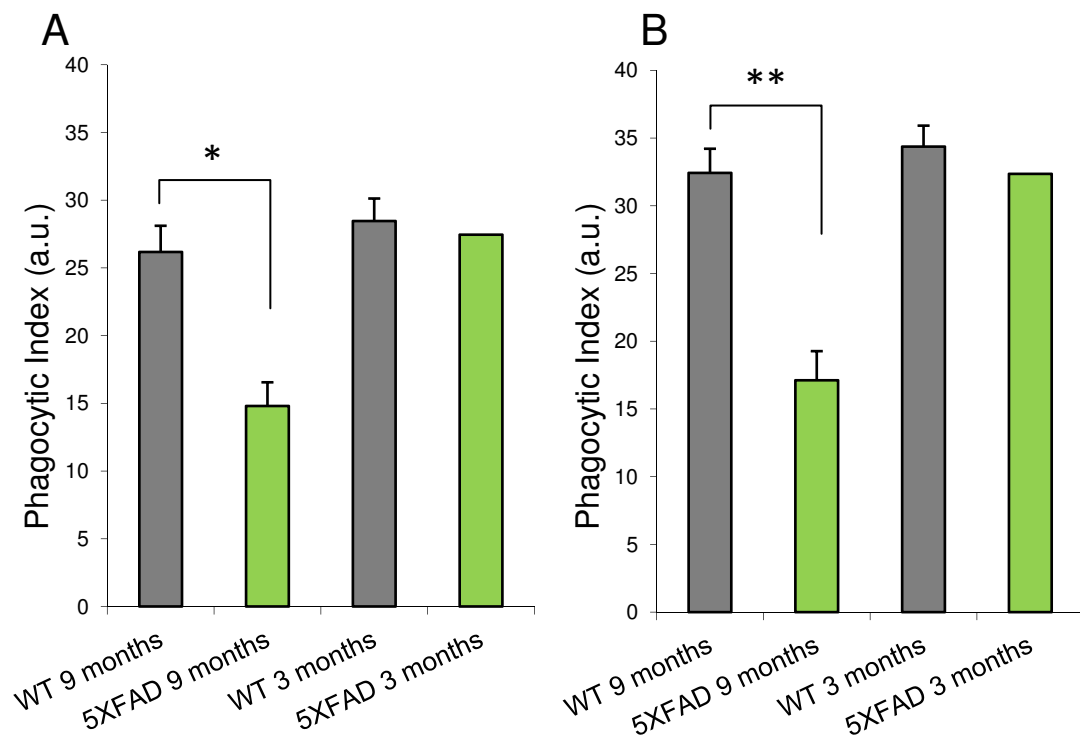


Fig.9. Determined phagocytic index of microglia *in situ*. The phagocytic index was calculated in two ways, in form of a group analysis (A) and as a single analysis (B). In both ways microglia of 9-month-old 5XFAD mice demonstrated a significant impairment in phagocytosis in contrast to age-matched WT controls (n=3 per genotype). Preliminary data on the phagocytic index of one 3 month old 5XFAD mouse in comparison to two WT controls suggests that microglia in 5XFAD mice have not developed this phenotype at 3 months of age. Data are mean \pm SEM, * $p=0.01-0.05$, ** $p=0.001-0.01$.

Preliminary results from this assay conducted with acute slices from 3-month-old 5XFAD (n=1) and WT mice (n=2), did not show the same trend (Fig.9).

There was an almost equal phagocytic activity between TG mice and controls at this age stage (28.460 a.u. vs. 27.451 a.u.). Quite contrary to the data at 9 month of age, the younger TG mice displayed a slightly higher readiness to phagocyte FBS-coated beads.

4. Discussion

According to the World Alzheimer Report (Prince et al., 2014) 50-75% of the 44 Mio. people living with dementia are affected by AD. It is a progressive neurodegenerative disease probably starting years before the onset of first symptoms and despite all scientific effort AD is still incurable. A small proportion of all AD cases develop symptoms already in their thirties, forties and fifties, but for the most part AD represents a disease of age. In this context the financial and social impact an aging population will have on the world health system is not neglectable. This will create an unconditional need for further research to develop new pharmacological treatments.

Over decades the focus on microglia has increased in AD research and these cells are nowadays considered to present an integral part of AD pathophysiology (Heppner et al., 2015). Several lines of evidence suggest that the A β plaques accumulated in AD patients trigger a sustained inflammatory response in microglia contributing to a loss of neurons and synapses (Prokop et al., 2013). Activated microglia are found in substantial numbers around A β plaques in AD (Bacscai et al., 2001; Itagaki et al., 1989) and the A β peptide itself seems to have an activating effect on microglia (Lue et al., 2001a).

The present work aimed at characterizing A β plaque-associated microglia in the 5XFAD mouse in respect to their membrane properties, purinergic responsiveness and phagocytic activity. To assess changes in these attributes over time 1-, 3- and 9-month-old animals were used in a mainly electrophysiological approach.

4.1 Microglia in the 5XFAD mouse get increasingly activated with age

Findings from other diseases suggest that some kind of activation in microglia can be reflected in their membrane properties (Avignone et al., 2008; Boucsein et al., 2000; Lyons et al., 2000), but until now the membrane current characteristics of microglia in and around A β plaques has not been assessed. The membrane properties of microglia directly linked to dense-core plaques in the 5XFAD mouse were analyzed by a series of hyper- and depolarizing voltage steps ranging between -170 mV to 60 mV. At 1 month of age microglia of 5XFAD and of WT mice did demonstrate similar current densities. However, the mean current density in microglia of 5XFAD at 3

months of age was significantly elevated in contrast to the density determined at 1 month of age, and again increased at 9 months of age (Fig.4A). Both, inward and outward current densities were affected, while the current densities in microglia of WT animals showed only insignificant increases with age, which were limited to the inward rectifying currents (Fig.4B).

Electrophysiological recordings of microglia in mouse models of SE, facial nerve axotomy or stroke (Avignone et al., 2008; Boucsein et al., 2000; Lyons et al., 2000) suggest that their activation follows a predetermined pattern. Shortly after activation microglia demonstrate enhanced inward currents in relation to control levels, which are later accompanied by increased outward currents. A similar pattern has been confirmed now for microglia in an AD mouse model (Fig.5) over a time span capturing the development of AD-related phenotypic changes (Oakley, 2006). Interestingly, in two studies (Boucsein, 2000; Avignone, 2008) this activation-related increase in inward and outward currents in microglia was followed by a return to control levels. Here it was clearly shown that microglia in the 5XFAD mouse remained on an activated level, which fits well to the concept of chronically activated microglia in AD (Heppner et al., 2015).

Chung et al. (2001) showed that A β induced significantly increased voltage-gated outward K⁺ currents, but not inward rectifying currents in cultured microglia. Thus, it seems that A β specifically elicits an outward current in microglia. It might be that microglia react differentially to their activation by different substances, which could be reflected in their voltage-gated membrane currents.

Furthermore, it can be assumed that the slight increase in inward currents from 1 to 9 months in WT microglia is a physiological consequence of age. It has recently been reported that cells undergo a change in their voltage-gated K⁺ channel expression leading to a increased inward and outward rectifier K⁺ current (Schilling et al., 2015).

In the future a further electrophysiological characterization of microglia in different mouse models will hopefully shed light on the involvement of increased membrane currents in diseases. In addition it has to be investigated whether microglia display a specific membrane current pattern upon exposure to different stimuli and whether this leads to a certain response in their immune functions.

4.2 Microglia in the 5XFAD mouse demonstrate a decreased responsiveness to purinergic signaling with age

An important danger signal in the brain is ATP binding to diverse P2 receptors in the brain. P2X7 upregulation in microglia has been linked to AD pathology and possibly to an activated state in these cells (McLarnon et al., 2006; Parvathenani et al., 2003; Rampe et al., 2004; Sanz et al., 2009). To assess the purinergic responses in microglia on an electrophysiological level, ATP or BzATP were applied to the bath during a series of hyper- and depolarizing voltage pulses. ATP and BzATP elicited similar current responses in microglia of 5XFAD and WT mice. With advancing age the membrane currents in microglia patched in the 5XFAD mice diminished for both, ATP (Fig.6A) and BzATP (Fig.6C). Similar trends were seen in WT animals (Fig.6B, Fig.6D) without statistical significance.

This finding contradicts the reported P2X7 receptor upregulation in AD (McLarnon et al., 2006). Although the P2X7 receptor immunoreactivity was found throughout the brain, it was predominantly expressed around A β plaques. However this experiment lacked direct evidence for the upregulation of the P2X7 receptor in plaque-associated microglia since a colocalization between microglia and the receptor was done in a separate experiment. Hence, it could either be that the P2X7 receptors expressed in microglia become non-functional over time or the receptor expression is not upregulated in microglia around A β plaques. Both, the P2X7 receptor upregulation in rat microglia (McLarnon et al., 2006), as well as the increase in electrophysiological responses in microglia upon ATP application (Avignone et al., 2008) were both conducted in hippocampal slices. Recordings of the present study were gained from cortical microglia, which could explain this contradiction.

Although the differences in ATP/BzATP-induced microglial membrane currents between the TG and WT mice did not reach significance (Fig.7), still there seem to be differences between these groups. It has to be noted, that the currents in microglia at 1 month of age were larger in 5XFAD mice than the currents in WT mice, a situation that was conversed in microglia at 3 and 9 months of age. A behavioral study on microglia *in situ* revealed that aging microglia demonstrated an impaired responsiveness to ATP application in relation to younger mice (Damani et al., 2011).

This suggests that both, a pathological and age-related, physiological effect accounts for the decreased responsiveness of microglia to ATP and BzATP seen in 5XFAD mice.

4.3 Microglia of 5XFAD experience an impairment in phagocytosis with age

Functionally, an activated phenotype of microglia is associated with increased phagocytic activity. Microglia get activated by A β and are principally competent to detect, incorporate and digest A β peptides (Frautschy et al., 1992; Weldon et al., 1998). Therefore the question arises why microglia obviously fail to successfully clear A β deposits in AD. Incubating acute brain slices from 9-month-old TG animals with FBS-labeled beads showed a clear impairment in phagocytosis in contrast to controls (Fig.9). This is consistent with the phagocytic capacities reported for two other AD mouse models (Krabbe et al., 2003). While microglia in the 4-month-old APPPS1 mice demonstrated a comparable impairment in phagocytosis, this was not seen in microglia of 3-month-old 5XFAD mice of the present study. Phagocytic capacities of microglia in 5XFAD mice at 3 months of age were comparable to WT levels. Importantly, phagocytic indices of microglia at different ages were all compared to levels in TG mice at 7-9 weeks of age. Given that this is the time when amyloid deposition has just started in the APPPS1 mouse (Radde, 2006), microglia might be activated due to A β deposits, but were not exposed to the damaging effects of A β for too long to impair their function.

It can be assumed that microglia in the 5XFAD mouse experience a phenomenon called "frustrated phagocytosis" (Khoury et al., 2008). It states that microglia, which are unable to remove all A β from the brain start to constantly secrete deleterious amounts of pro-inflammatory molecules. Hickman et al. (2008) demonstrated that mRNA levels of cytokines increased with age, while proteins involved in phagocytosis decreased with age in an AD mouse model. In accordance with this proinflammatory cytokines were shown to inhibit microglial phagocytosis of fA β *in vitro* (Koenigsknecht-Talboo, 2005), while a non-steroidal anti-inflammatory drug attenuated AD pathology *in vivo* (Lim et al., 2000). Considering these data it can be assumed that the activated state itself leads to the impairment in phagocytosis at a certain point. In the future the relationship between microglial membrane currents

and decreased phagocytic activity in AD mouse models needs to be investigated more deeply.

4.4 Microglia in the 5XFAD might undergo senescence

The present study not only shows for the first time that microglia undergo dramatic changes in their membrane properties in an AD mouse model, but that the same cell type experiences an altered electrophysiological responsiveness to ATP and BzATP with age, partly caused by normal physiological developments. The impairment of microglial phagocytosis and electrophysiological changes in 5XFAD mice coincide with a decreased responsiveness to P2X7 receptor agonists, indicating a correlation between these two parameters. As contradictory these findings seem on first glance, they accommodate well considering the microglial senescence hypothesis (Streit et al., 2014). It states that dysfunctional microglia next to chronic neuroinflammation contribute substantially to age-related neurodegenerative diseases like AD. Histopathological investigations on brains from patients with AD and Down's syndrome pathology showed that degenerating neuronal structures were rather associated with dystrophic (senescent cells) than activated microglia (Streit et al., 2009). Considering the gradual activation scheme for microglia in AD (Fig.10) proposed by Prokop et al. (2013), it can be assumed that the increasing activation of microglia is reflected in their voltage-gated membrane currents. Diminishing electrophysiological responses to purinergic signaling could demonstrate the progressive dysfunctional state of microglia. This state could be linked to the permanent activation of outward currents, which accumulates in the functional impairment of microglia. It is highly likely that a significant population of microglia are in a dystrophic state already at 9 months of age. Since this is the age at which significant neuronal loss starts in the 5XFAD mouse (Eimer et al., 2013; Oakley et al., 2006), they might lose their neurosupportive function (Nakajima et al., 2004) much earlier. It has been published recently that ATP levels in an AD mouse model were significantly reduced in contrast to control levels at 5 months of age indicating ROS production and mitochondrial dysfunction (Zhang et al., 2015).

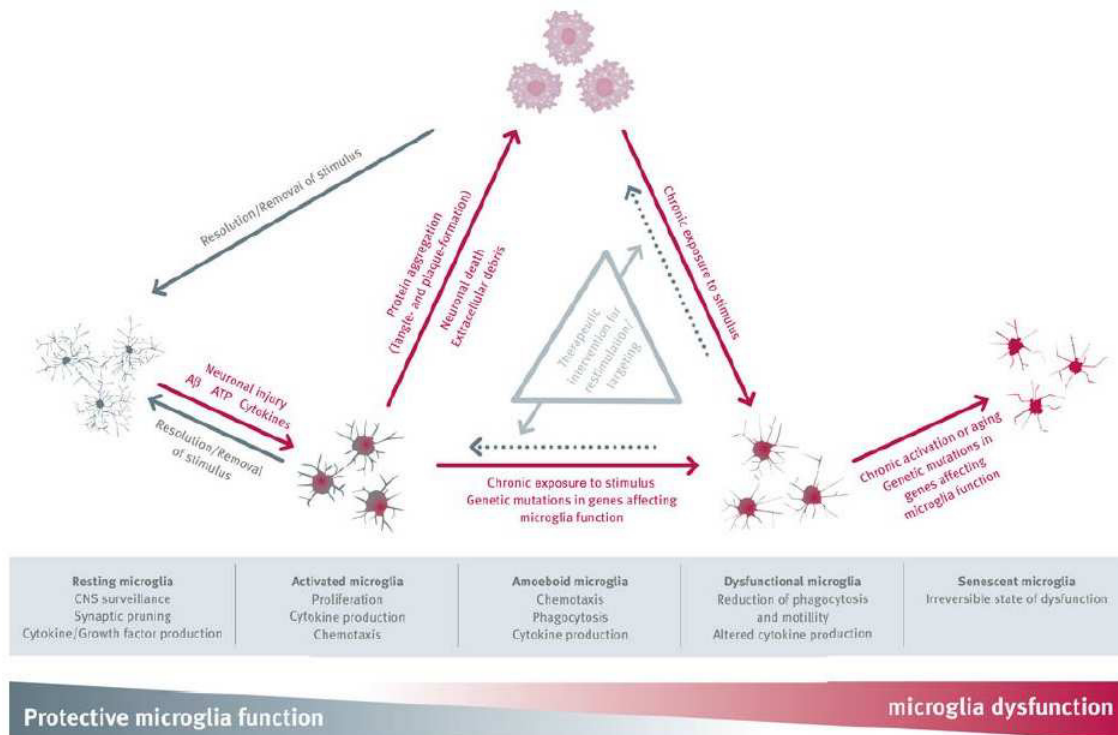


Fig.10. A basic scheme depicting the main stages of microglial state induced by the environmental setting. Ramified (resting) microglia scan their environment for danger signal, engage in developmental processes and maintain the homeostasis of the brain. Due to external triggers microglia can become activated, which causes them to proliferate and produce cytokines as well as chemokines as an immunological response. In order to exert their phagocytic functions microglia become amoeboid and move to the site of harm, where they continue to secrete pro-inflammatory cytokines. As soon as the damage or pathogen is eradicated microglia return to their surveillance function. In a chronic state microglia become dysfunctional and lose their normal (benign) function. While this state is still reversible, senescence is not. Figure taken from Prokop et al. (2013). Microglia actions in Alzheimer’s disease. *Acta Neuropathologica*, 126(4), 461–477.

Furthermore, it has to be stressed, that age-related changes seem to contribute to pathologic changes in the 5XFAD mouse model. This is important since the senescence hypothesis attributes an increased susceptibility of the CNS to develop neurodegenerative diseases to the emergence of dystrophic and therefore dysfunctional microglia (Streit et al., 2014). The microglial population in the CNS is maintained throughout life, which undergoes local proliferation in the case of disease (Ajami et al., 2007). Consequently, microglia are subject to a natural aging process, which may cause dysfunction under certain circumstances. Microglia in aged mice and in disease share many characteristics. They increase in number and density, are less

evenly distributed than in young mice, and lose their ramified morphology seen in younger animals (Wong, 2013). Moreover, microglia in aging brains upregulate genes known as markers for activated microglia like major histocompatibility complex II (MHC II), CD86, MHC II transcriptional activator (CIITA) and interferon gamma (INF- γ) (Rogers et al., 1988; Frank et al., 2006).

In conclusion, this work provides important data on changes in membrane properties and phagocytic function in a mouse model of AD during the emergence of the main pathological phenotype. Furthermore, it underlines the importance of investigating age-related alterations of microglia characteristics and their roles and effects in the development of AD.

5. References

- Ajami, B., Bennett, J. L., Krieger, C., Tetzlaff, W., & Rossi, F. M. V. (2007). Local self-renewal can sustain CNS microglia maintenance and function throughout adult life. *Nature Neuroscience*, *10*(12), 1538–1543. <http://doi.org/10.1038/nn2014>
- Akiyama, H. (1994). Inflammatory response in Alzheimer's disease. *The Tohoku Journal of Experimental Medicine*, *174*(3), 295–303.
- Alzheimer, A. (1907). Über eine eigenartige Erkrankung der Hirnrinde. *Allgemeine Zeitschrift für Psychiatrie und psychisch-gerichtliche Medizin* *64*, 146 -148.
- Amor, S., Puentes, F., Baker, D., & van der Valk, P. (2010). Inflammation in neurodegenerative diseases. *Immunology*, *129*(2), 154–169. <http://doi.org/10.1111/j.1365-2567.2009.03225.x>
- Ard, M. D., Cole, G. M., Wei, J., Mehrle, A. P., & Fratkin, J. D. (1996). Scavenging of Alzheimer's Amyloid -Protein by Microglia in Culture. *Journal of Neuroscience Research*, *43*(2), 190–202.
- Avignone, E., Ulmann, L., Levavasseur, F., Rassendren, F., & Audinat, E. (2008). Status Epilepticus Induces a Particular Microglial Activation State Characterized by Enhanced Purinergic Signaling. *Journal of Neuroscience*, *28*(37), 9133–9144. <http://doi.org/10.1523/JNEUROSCI.1820-08.2008>
- Bacskai, B. J., Kajdasz, S. T., Christie, R. H., Carter, C., Games, D., Seubert, P., ... Hyman, B. T. (2001). Imaging of amyloid- β deposits in brains of living mice permits direct observation of clearance of plaques with immunotherapy. *Nature Medicine*, *7*(3), 369–372.
- Bard, F., Cannon, C., Barbour, R., Burke, R.-L., Games, D., Grajeda, H., ... others. (2000). Peripherally administered antibodies against amyloid β -peptide enter the central nervous system and reduce pathology in a mouse model of Alzheimer disease. *Nature Medicine*, *6*(8), 916–919.
- Boucsein, C., Kettenmann, H., & Nolte, C. (2000). Electrophysiological properties of microglial cells in normal and pathologic rat brain slices. *European Journal of Neuroscience*, *12*(6), 2049–2058. <http://doi.org/10.1046/j.1460-9568.2000.00100.x>

- Boucsein, C., Zacharias, R., Farber, K., Pavlovic, S., Hanisch, U.-K., & Kettenmann, H. (2003). Purinergic receptors on microglial cells: functional expression in acute brain slices and modulation of microglial activation in vitro. *European Journal of Neuroscience*, *17*(11), 2267–2276. <http://doi.org/10.1046/j.1460-9568.2003.02663.x>
- Chung, S., Lee, J., Joe, E.-H., & Uhm, D.-Y. (2001). β -amyloid peptide induces the expression of voltage dependent outward rectifying K⁺ channels in rat microglia. *Neuroscience Letters*, *300*(2), 67–70. [http://doi.org/10.1016/S0304-3940\(01\)01516-6](http://doi.org/10.1016/S0304-3940(01)01516-6)
- Damani, M. R., Zhao, L., Fontainhas, A. M., Amaral, J., Fariss, R. N., & Wong, W. T. (2011). Age-related alterations in the dynamic behavior of microglia: Age-related changes in microglial behavior. *Aging Cell*, *10*(2), 263–276. <http://doi.org/10.1111/j.1474-9726.2010.00660.x>
- Davalos, D., Grutzendler, J., Yang, G., Kim, J. V., Zuo, Y., Jung, S., ... Gan, W.-B. (2005). ATP mediates rapid microglial response to local brain injury in vivo. *Nature Neuroscience*, *8*(6), 752–758. <http://doi.org/10.1038/nn1472>
- D Skaper, S. (2011). Ion channels on microglia: therapeutic targets for neuroprotection. *CNS & Neurological Disorders-Drug Targets (Formerly Current Drug Targets-CNS & Neurological Disorders)*, *10*(1), 44–56.
- Eimer, W. A., & Vassar, R. (2013). Neuron loss in the 5XFAD mouse model of Alzheimer's disease correlates with intraneuronal A β 42 accumulation and Caspase-3 activation. *Mol Neurodegener*, *8*(2). Retrieved from <http://www.biomedcentral.com/content/pdf/1750-1326-8-2.pdf>
- Frank, M. G., Barrientos, R. M., Biedenkapp, J. C., Rudy, J. W., Watkins, L. R., & Maier, S. F. (2006). mRNA up-regulation of MHC II and pivotal pro-inflammatory genes in normal brain aging. *Neurobiology of Aging*, *27*(5), 717–722. <http://doi.org/10.1016/j.neurobiolaging.2005.03.013>
- Frautschy, S. A., Cole, G. M., & Baird, A. (1992). Phagocytosis and deposition of vascular beta-amyloid in rat brains injected with Alzheimer beta-amyloid. *The American Journal of Pathology*, *140*(6), 1389.

- Frautschy, S. A., Yang, F., Irrizarry, M., Hyman, B., Saido, T. C., Hsiao, K., & Cole, G. M. (1998). Microglial response to amyloid plaques in APPsw transgenic mice. *The American Journal of Pathology*, *152*(1), 307.
- Gao, H.-M., & Hong, J.-S. (2008). Why neurodegenerative diseases are progressive: uncontrolled inflammation drives disease progression. *Trends in Immunology*, *29*(8), 357–365. <http://doi.org/10.1016/j.it.2008.05.002>
- Grathwohl, S. A., Kälin, R. E., Bolmont, T., Prokop, S., Winkelmann, G., Kaeser, S. A., ... Jucker, M. (2009). Formation and maintenance of Alzheimer's disease β -amyloid plaques in the absence of microglia. *Nature Neuroscience*, *12*(11), 1361–1363. <http://doi.org/10.1038/nn.2432>
- Haass, C., Kaether, C., Thinakaran, G., & Sisodia, S. (2012). Trafficking and Proteolytic Processing of APP. *Cold Spring Harbor Perspectives in Medicine*, *2*(5), a006270–a006270. <http://doi.org/10.1101/cshperspect.a006270>
- Heppner, F. L., Ransohoff, R. M., & Becher, B. (2015). Immune attack: the role of inflammation in Alzheimer disease. *Nature Reviews Neuroscience*, *16*(6), 358–372. <http://doi.org/10.1038/nrn3880>
- Hickman, S. E., Allison, E. K., & Khoury, J. El. (2008). Microglial Dysfunction and Defective β -Amyloid Clearance Pathways in Aging Alzheimer's Disease Mice. *Journal of Neuroscience*, *28*(33), 8354–8360. <http://doi.org/10.1523/JNEUROSCI.0616-08.2008>
- Hide, I., Tanaka, M., Inoue, A., Nakajima, K., Kohsaka, S., Inoue, K., & Nakata, Y. (2000). Extracellular ATP Triggers Tumor Necrosis Factor- α Release from Rat Microglia. *Journal of Neurochemistry*, *75*(3), 965–972.
- Itagaki, S., McGeer, P. L., Akiyama, H., Zhu, S., & Selkoe, D. (1989). Relationship of microglia and astrocytes to amyloid deposits of Alzheimer Disease. *Journal of Neuroimmunology*, *24*(3), 173–182.
- Kettenmann, H., Hanisch, U.-K., Noda, M., & Verkhratsky, A. (2011). Physiology of Microglia. *Physiological Reviews*, *91*(2), 461–553. <http://doi.org/10.1152/physrev.00011.2010>
- Kettenmann, H., Hoppe, D., Gottmann, K., Banati, R., Kreutzberg, G. (1990). Cultured Microglial Cells Have a Distinct Pattern of Membrane Channels Different From Peritoneal Macrophages. *Journal of Neuroscience* *26*, 278-287.

- Khoury, J. E., & Luster, A. D. (2008). Mechanisms of microglia accumulation in Alzheimer's disease: therapeutic implications. *Trends in Pharmacological Sciences*, 29(12), 626–632. <http://doi.org/10.1016/j.tips.2008.08.004>
- Koenigsknecht-Talboo, J. (2005). Microglial Phagocytosis Induced by Fibrillar -Amyloid and IgGs Are Differentially Regulated by Proinflammatory Cytokines. *Journal of Neuroscience*, 25(36), 8240–8249. <http://doi.org/10.1523/JNEUROSCI.1808-05.2005>
- Koizumi, S., Shigemoto-Mogami, Y., Nasu-Tada, K., Shinozaki, Y., Ohsawa, K., Tsuda, M., ... Inoue, K. (2007). UDP acting at P2Y6 receptors is a mediator of microglial phagocytosis. *Nature*, 446(7139), 1091–1095. <http://doi.org/10.1038/nature05704>
- Krabbe, G., Halle, A., Matyash, V., Rinnenthal, J. L., Eom, G. D., Bernhardt, U., ... Heppner, F. L. (2013). Functional Impairment of Microglia Coincides with Beta-Amyloid Deposition in Mice with Alzheimer-Like Pathology. *PLoS ONE*, 8(4), e60921. <http://doi.org/10.1371/journal.pone.0060921>
- Krstic, D., Madhusudan, A., Doehner, J., Vogel, P., Notter, T., Imhof, C., ... others. (2012). Systemic immune challenges trigger and drive Alzheimer-like neuropathology in mice. *Journal of Neuroinflammation*, 9(1), 151.
- Lee, C. Y. D., & Landreth, G. E. (2010). The role of microglia in amyloid clearance from the AD brain. *Journal of Neural Transmission*, 117(8), 949–960. <http://doi.org/10.1007/s00702-010-0433-4>
- Lim, G. P., Yang, F., Chu, T., Chen, P., Beech, W., Teter, B., ... others. (2000). Ibuprofen suppresses plaque pathology and inflammation in a mouse model for Alzheimer's disease. *The Journal of Neuroscience*, 20(15), 5709–5714.
- Lue, L.-F., Rydel, R., Brigham, E. F., Yang, L.-B., Hampel, H., Murphy, G. M., ... others. (2001a). Inflammatory repertoire of Alzheimer's disease and nondemented elderly microglia in vitro. *Glia*, 35(1), 72–79.
- Lue, L.-F., Walker, D. G., & Rogers, J. (2001b). Modeling microglial activation in Alzheimer's disease with human postmortem microglial cultures. *Neurobiology of Aging*, 22(6), 945–956.
- Lyons, S. A., Pastor, A., Ohlemeyer, C., Kann, O., Wiegand, F., Prass, K., ... Dirnagl, U. (2000). Distinct physiologic properties of microglia and blood-borne cells in rat

- brain slices after permanent middle cerebral artery occlusion. *Journal of Cerebral Blood Flow & Metabolism*, 20(11), 1537–1549.
- Maezawa, I., Zimin, P. I., Wulff, H., & Jin, L.-W. (2011). Amyloid- Protein Oligomer at Low Nanomolar Concentrations Activates Microglia and Induces Microglial Neurotoxicity. *Journal of Biological Chemistry*, 286(5), 3693–3706. <http://doi.org/10.1074/jbc.M110.135244>
- Malm, T. M., Koistinaho, M., Pärepallo, M., Vatanen, T., Ooka, A., Karlsson, S., & Koistinaho, J. (2005). Bone-marrow-derived cells contribute to the recruitment of microglial cells in response to β -amyloid deposition in APP/PS1 double transgenic Alzheimer mice. *Neurobiology of Disease*, 18(1), 134–142. <http://doi.org/10.1016/j.nbd.2004.09.009>
- McGeer, P. L., Klegeris, A., Walker, D. G., Yasuhara, O., & McGeer, E. G. (1994). Pathological proteins in senile plaques. *The Tohoku Journal of Experimental Medicine*, 174(3), 269–277.
- McLarnon, J. G., Ryu, J. K., Walker, D. G., & Choi, H. B. (2006). Upregulated Expression of Purinergic P2X7 Receptor in Alzheimer Disease and Amyloid- β Peptide-Treated Microglia and in Peptide-Injected Rat Hippocampus: *Journal of Neuropathology and Experimental Neurology*, 65(11), 1090–1097. <http://doi.org/10.1097/01.jnen.0000240470.97295.d3>
- McLellan, M. E., Kajdasz, S. T., Hyman, B. T., Bacskai, B. J. (2003). In Vivo Imaging of Reactive Oxygen Species Specifically Associated with Thioflavine S-Positive Amyloid Plaques by Multiphoton Microscopy. *The Journal of Neuroscience*, 23(6), 2212-2217.
- Monif, M., Burnstock, G., & Williams, D. A. (2010). Microglia: Proliferation and activation driven by the P2X7 receptor. *The International Journal of Biochemistry & Cell Biology*, 42(11), 1753–1756. <http://doi.org/10.1016/j.biocel.2010.06.021>
- Mrak, R. E. (2012). Microglia in Alzheimer Brain: A Neuropathological Perspective. *International Journal of Alzheimer's Disease*, 2012, 1–6. <http://doi.org/10.1155/2012/165021>

- Nakajima, K., & Kohsaka, S. (2004). Microglia: neuroprotective and neurotrophic cells in the central nervous system. *Current Drug Targets-Cardiovascular & Hematological Disorders*, 4(1), 65–84.
- Nörenberg, W., Gebicke-Haerter, P. J., Illes, P. (1992). Inflammatory stimuli induce a new K⁺ outward current in cultured rat microglia. *Neuroscience Letters*, 147, 171-174.
- Oakley, H., Cole, S. L., Logan, S., Maus, E., Shao, P., Craft, J., ... Vassar, R. (2006). Intraneuronal beta-Amyloid Aggregates, Neurodegeneration, and Neuron Loss in Transgenic Mice with Five Familial Alzheimer's Disease Mutations: Potential Factors in Amyloid Plaque Formation. *Journal of Neuroscience*, 26(40), 10129–10140. <http://doi.org/10.1523/JNEUROSCI.1202-06.2006>
- Ohgami, T., Kitamoto, T., Shin, R. W., Kaneko, Y., Ogomori, K., & Tateishi, J. (1991). Increased senile plaques without microglia in Alzheimer's disease. *Acta Neuropathologica*, 81(3), 242–247.
- Ohsawa, K., Irino, Y., Nakamura, Y., Akazawa, C., Inoue, K., & Kohsaka, S. (2007). Involvement of P2X₄ and P2Y₁₂ receptors in ATP-induced microglial chemotaxis. *Glia*, 55(6), 604–616. <http://doi.org/10.1002/glia.20489>
- Parvathenani, L. K., Tertyshnikova, S., Greco, C. R., Roberts, S. B., Robertson, B., & Posmantur, R. (2003). P2X₇ Mediates Superoxide Production in Primary Microglia and Is Up-regulated in a Transgenic Mouse Model of Alzheimer's Disease. *Journal of Biological Chemistry*, 278(15), 13309–13317. <http://doi.org/10.1074/jbc.M209478200>
- Pont-Lezica, L., Béchade, C., Belarif-Cantaut, Y., Pascual, O., & Bessis, A. (2011). Physiological roles of microglia during development: Developmental roles of microglia. *Journal of Neurochemistry*, 119(5), 901–908. <http://doi.org/10.1111/j.1471-4159.2011.07504.x>
- Prince, M., Albanese, E., Guerchet, M., Prina, M. (2014). World Alzheimer Report 2014. Dementia and Risk Reduction.
- Prince, M., Wimo, A., Guerchet, M., All, G.-C., Wu,, Y.-T., Prina, M. (2015). World Alzheimer Report 2015. The Global Impact of Dementia.

- Prokop, S., Miller, K. R., & Heppner, F. L. (2013). Microglia actions in Alzheimer's disease. *Acta Neuropathologica*, *126*(4), 461–477. <http://doi.org/10.1007/s00401-013-1182-x>
- Rampe, D., Wang, L., & Ringheim, G. E. (2004). P2X7 receptor modulation of β -amyloid- and LPS-induced cytokine secretion from human macrophages and microglia. *Journal of Neuroimmunology*, *147*(1-2), 56–61. <http://doi.org/10.1016/j.jneuroim.2003.10.014>
- Rock, R. B., Gekker, G., Hu, S., Sheng, W. S., Cheeran, M., Lokensgard, J. R., & Peterson, P. K. (2004). Role of Microglia in Central Nervous System Infections. *Clinical Microbiology Reviews*, *17*(4), 942–964. <http://doi.org/10.1128/CMR.17.4.942-964.2004>
- Rogers, J., Lubner-Narod, J., Styren, S. D., Civin, W. H. (1988). Expression of Immune-Associated Antigens by Cells of the Human Central Nervous System: Relationship to the Pathology of Alzheimer's Disease. *Neurobiology of Aging*, *9*, 339-349.
- Rogers, J., & Lue, L.-F. (2001). Microglial chemotaxis, activation, and phagocytosis of amyloid β -peptide as linked phenomena in Alzheimer's disease. *Neurochemistry International*, *39*, 333-340.
- Salminen, A., Ojala, J., Kauppinen, A., Kaarniranta, K., & Suuronen, T. (2009). Inflammation in Alzheimer's disease: Amyloid- β oligomers trigger innate immunity defence via pattern recognition receptors. *Progress in Neurobiology*, *87*(3), 181–194. <http://doi.org/10.1016/j.pneurobio.2009.01.001>
- Sanz, J. M., Chiozzi, P., Ferrari, D., Colaianna, M., Idzko, M., Falzoni, S., ... Di Virgilio, F. (2009). Activation of Microglia by Amyloid Requires P2X7 Receptor Expression. *The Journal of Immunology*, *182*(7), 4378–4385. <http://doi.org/10.4049/jimmunol.0803612>
- Sasmono, R. T., O'Ceandly, D., Pollard, J. W., Tong, W., Pavli, P., Wainwright, B. J., ... Hume, D. A. (2003). A macrophage colony-stimulating factor receptor–green fluorescent protein transgene is expressed throughout the mononuclear phagocyte system of the mouse. *Blood*, *101*(3), 1155–1163.

- Schilling, T., & Eder, C. (2015). Microglial K⁺ channel expression in young adult and aged mice: K⁺ Channels in Young Adult and Aged Microglia. *Glia*, *63*(4), 664–672. <http://doi.org/10.1002/glia.22776>
- Shaffer, L. M., Dority, M. D., Gupta-Bansal, R., Frederickson, R. C. A., Younkin, S. G., & Brunden, K. R. (1995). Amyloid β Protein (A β) Removal by Neuroglial Cells in Culture. *Neurobiology of Aging*, *16*(5), 737-745.
- Skaper, S. D., Debetto, P., & Giusti, P. (2010). The P2X7 purinergic receptor: from physiology to neurological disorders. *The FASEB Journal*, *24*(2), 337–345. <http://doi.org/10.1096/fj.09-138883>
- Sperlágh, B., & Illes, P. (2007). Purinergic modulation of microglial cell activation. *Purinergic Signalling*, *3*(1-2), 117–127. <http://doi.org/10.1007/s11302-006-9043-x>
- Stanley, E. R., Berg, K. L., Einstein, D. B., Lee, P. S., Pixley, F. J., Wang, Y., & Yeung, Y.-G. (1997). Biology and action of colony-stimulating factor-1. *Molecular Reproduction and Development*, *46*(1), 4–10.
- Streit, W. J., Braak, H., Xue, Q.-S., & Bechmann, I. (2009). Dystrophic (senescent) rather than activated microglial cells are associated with tau pathology and likely precede neurodegeneration in Alzheimer's disease. *Acta Neuropathologica*, *118*(4), 475–485. <http://doi.org/10.1007/s00401-009-0556-6>
- Streit, W. J., Xue, Q.-S., Tischer, J., & Bechmann, I. (2014). Microglial pathology. *Acta Neuropathol Commun*, *2*(1), 142.
- Tanzi, R. E., & Bertram, L. (2005). Twenty Years of the Alzheimer's Disease Amyloid Hypothesis: A Genetic Perspective. *Cell*, *120*(4), 545–555. <http://doi.org/10.1016/j.cell.2005.02.008>
- Tarkowski, E., Andreasen, N., Tarkowski, A., & Blennow, K. (2003). Intrathecal inflammation precedes development of Alzheimer's disease. *Journal of Neurology, Neurosurgery & Psychiatry*, *74*(9), 1200–1205.
- Terry, R. D., Gonatas, N. K., & Weiss, M. (1964). Ultrastructural studies in Alzheimer's presenile dementia. *The American Journal of Pathology*, *44*(2), 269.
- Uchihara, T., Nakamura, A., Yamazaki, M., & Mori, O. (2000). Tau-positive neurons in corticobasal degeneration and Alzheimer's disease—distinction by thiazin red and silver impregnations. *Acta Neuropathologica*, *100*(4), 385–389.

- Weldon, D. T., Rogers, S. D., Ghilardi, J. R., Finke, M. P., Cleary, J. P., O'Hare, E., Esler, W. P., Maggio, J. E., Mantyh, P. W. (1998). Fibrillar β -Amyloid Induces Microglial Phagocytosis, Expression of Inducible Nitric Oxid Synthase, and Loss of a Select Population of Neurons in the Rat CNS In Vivo. *The Journal of Neuroscience*, *18*(6), 2161–2173.
- Wilkinson, K., & Khoury, J. El. (2012). Microglial Scavenger Receptors and Their Roles in the Pathogenesis of Alzheimer's Disease. *International Journal of Alzheimer's Disease*, *2012*, 1–10. <http://doi.org/10.1155/2012/489456>
- Wong, W. T. (2013). Microglial aging in the healthy CNS: phenotypes, drivers, and rejuvenation. *Frontiers in Cellular Neuroscience*, *7*. <http://doi.org/10.3389/fncel.2013.00022>
- Yang, R., & Liang, B. T. (2012). Cardiac P2X4 Receptors: Targets in Ischemia and Heart Failure? *Circulation Research*, *111*(4), 397–401. <http://doi.org/10.1161/CIRCRESAHA.112.265959>
- Zhang, C., Rissman, R. A., & Feng, J. (2015). Characterization of ATP Alternations in an Alzheimer's Transgenic Mouse Model. *Journal of Alzheimer's Disease: JAD*, *44*(2), 375.

6. Abstract

One of the central hallmarks of AD is the presence of insoluble β -Amyloid ($A\beta$) deposits. Brains of AD patients are characterized by microgliosis around $A\beta$ dense-core plaques and upregulated levels of inflammation. Several studies suggest that microglia activated by the $A\beta$ peptide present the source of inflammation contributing to neurodegeneration. Although much effort was put into the assessment of the cell membrane receptors and secretory products involved in the AD pathology, $A\beta$ -associated microglia lack an electrophysiological characterization. There is good evidence that an activation of microglia is reflected in their membrane currents and that they increase in disease. ATP acts as a universal danger signal in the brain and an upregulation of purinergic receptors in microglia is assumed to be involved in AD. Furthermore activated microglia are principally able of $A\beta$ peptide phagocytosis but obviously fail to control the increasing accumulation of $A\beta$ plaques.

The membrane current pattern, the purinergic responsiveness and the phagocytic capacities of microglia were analyzed in the 5XFAD AD mouse model at 1, 3 and 9 months of age. Whole-cell recordings of $A\beta$ plaque-associated microglia in acute brain slices from 5XFAD mice demonstrated a significant increase in inward and outward current densities with age. Electrophysiological responses to ATP and BzATP led to similar currents in microglia of 5XFAD and control animals per age group, but diminished with age only in the 5XFAD mouse. The changes in electrophysiological properties correlated with an impairment of phagocytosis in microglia indicating a dysregulation in microglial function.

The present study shows for the first time that microglia in an AD mouse model undergo dramatic changes in their membrane properties reflecting their increasing activation. Diminishing electrophysiological responses to purinergic signaling could demonstrate the progressive dysfunctional state of microglia, which culminates in their functional impairment of phagocytosis.

7. Zusammenfassung

Die Alzheimer-Krankheit ist geprägt von extrazellulären Anhäufungen des β -Amyloid Peptides (Plaques). Die Gehirne von Alzheimer-Patienten sind außerdem gekennzeichnet von Mikroglia, die um senile Plaques herum zu finden sind, sowie von erhöhten Entzündungswerten. Zahlreiche Studien legen nahe, dass Mikroglia von dem β -Amyloid ($A\beta$) Peptid aktiviert werden und wesentlich an dem Entzündungsprozess und der Neurodegeneration beteiligt sind. Bislang wurden hauptsächlich Membranrezeptoren in Mikroglia und die von ihnen sezernierten Moleküle untersucht, doch die elektrophysiologischen Eigenschaften von diesen $A\beta$ -assoziierten Zellen vernachlässigt. Studien legen nahe, dass die Aktivierung von Mikroglia sich in ihren Membranströmen widerspiegelt, und dass diese im Krankheitsfall größer werden. ATP kann als universelles Gefahrensignal im Gehirn gewertet werden, und es wird angenommen, dass eine Hochregulierung von purinergen Rezeptoren in Mikroglia in der Alzheimer-Krankheit stattfindet. Des Weiteren sind Mikroglia grundsätzlich imstande $A\beta$ Peptide zu phagozytieren, aber schaffen es nicht die zunehmenden Plaqueablagerungen einzudämmen.

Die Membranströme, die purinergen Antworten und die phagozytischen Eigenschaften von Mikroglia wurden in der 5XFAD Alzheimer Modellmaus im Alter von 1, 3 und 9 Monaten analysiert. Ganzzelleableitungen von Plaque-assoziierten Mikroglia in frischen Hirnschnitten von 5XFAD Mäusen offenbarten eine deutlich Zunahme der Einwärts- und Auswärtsstromdichte mit zunehmendem Alter. Obwohl die elektrophysiologischen Antworten auf ATP und BzATP zu ähnlichen Strömen in Mikroglia von 5XFAD- und Kontrolltieren in jeder Altersgruppe führten, nahmen nur die Membranströme in den 5XFAD Mäusen mit zunehmendem Alter ab. Die Veränderung in den elektrophysiologischen Eigenschaften korrelierte mit einer verminderten phagozytischen Leistung in Mikroglia, was auf eine Dysregulierung in ihrer Funktion schließen lässt.

Diese Studie zeigt zum ersten Mal, dass Mikroglia in einem Alzheimer Mausmodell wesentliche Veränderungen ihrer Membraneigenschaften durchlaufen, was auf ihre zunehmende Aktivierung hindeutet. Abnehmende elektrophysiologische Antworten auf purinerge Moleküle steht indikativ für den fortschreitenden dysfunktionale Zustand von Mikroglia, was letztendlich im Verlust ihrer phagozytischen Funktionalität mündet.

8. List of abbreviations

a.u.	Arbitrary unit
ACSF	Artificial cerebrospinal fluid
AD	Alzheimer's Disease
APOE	Apolipoprotein E
APP	Amyloid precursor protein
A β	β -amyloid
ATP	Adenosine 5'-triphosphate
BSA	Bovine serum albumin
BzATP	2',3'-(benzoyl-4-benzoyl)-ATP
°C	Celsius
CNS	Central nervous system
DAMPs	Danger-associated molecular patterns
DKS	Donkey serum
EGFP	Enhanced green fluorescent protein
EOAD	Early-onset Alzheimer's Disease
EOFAD	Early-onset familial Alzheimer's Disease
FBS	Fetal bovine serum
hAPP	Human amyloid precursor protein
HBBS	Hank's balanced salt solution
Iba1	Inositol calcium-binding adapter molecule 1

IgG	Immunglobulin G
IL	Interleukin
LOAD	Late-onset Alzheimer's Disease
M	Molar
MCP-1	Monocyte chemoattractant protein-1
M-CSF	Macrophage colony-stimulating factor
ml	Milliliter
mM	Millimomolar
mV	Millivolt
MΩ	Megaohm
nA	Nanoampere
pA	Picoampere
PAMPs	Pathogen-associated molecular patterns
PB	Phosphate buffer
PBS	Phosphate-buffered saline
pF	Picofarad
PFA	Parafomaldehyde
pH	Potential hydrogen
PRR	Pattern-recognition receptors
PS-1	Presenilin 1
PS-2	Presenilin 2
ROS	Reactive oxygen species
RPM	Revolutions per minute
SEM	Standard error of the mean

TG	transgenic
TLRs	Toll-like receptors
TNF- α	Tumor necrosis factor α
WT	Wild-type
μ l	Microliter
μ m	Micrometer

9. Acknowledgements

I want to express my gratitude towards Prof. Dr. Helmut Kettenmann for giving me the opportunity to work in his lab and his support throughout this project.

Univ.-Prof. Dr. Johannes Berger I want to thank for agreeing to be my supervisor at the University of Vienna and supporting me throughout my study of Molecular Biology as the coordinator of Neuroscience.

I also want to express my gratitude towards Stefan Wendt, M.Sc. for teaching me the patch-clamp technique and being my personal advisor during the work on my master's project.

Furthermore I want to thank Niklas Meyer, Nadine Richter, Philipp Jordan and Frank Szulzewsky for giving me good advice regarding different methods in molecular biology.

Great thanks to all the people in the Kettenmann lab, and the persons, who keep it running: Birgit Jarchow, Regina Piske, Nadine Scharek and Michaela Seeger-Zografakis.

Also I want to thank Florian Hetsch for his loving support during the work on my master's thesis and my family, which has still not ostracized me despite my permanent absence.

10. Curriculum Vitae

PERSONAL INFORMATION

Natascha Vana

Sex female

Nationality Austria

EDUCATION AND TRAINING

October 2014 - July 2015

Master project

the Max Delbrück Center for Molecular Medicine (MDC) in Berlin, Germany

July - October 2014

Research Training Fellowship For Undergraduate Students

International School For Advanced Studies in Trieste, Italy

Since WS 2013

Master programme in Molecular Biology, Neuroscience

University of Vienna, Austria

SS 2013

Erasmus programme

University of Padova, Italy

WS 2012

Master programme in Anthropology

University of Vienna, Austria

SS 2008 - SS 2012

Bachelor programme in Biology, Anthropology

University of Vienna, Austria

WS 2007

Bachelor programme in Art History

University of Vienna, Austria

2003 - 2007

High School, Graduation with Distinction

Artistic Branch, Italian as a second foreign language

Oberstufenrealgymnasium ORG1 Hegelgasse 14, 1010 Vienna, Austria

1999 - 2003

Middle School, Focus on Natural Science

Bundesgymnasium GRG3 Hagenmüllergasse 30, 1030 Vienna, Austria

1995 - 1999

Elementary School

Volksschule Petrusgasse 10, 1030 Vienna, Austria